# Characterization of Mutations in the C-terminal Domain of the NS1 Protein of Influenza A Virus and Live Attenuated Influenza Vaccine

James E. Stanton

A thesis submitted to Johns Hopkins University in conformity with the requirements for

the degree for Master of Science

Baltimore, Maryland

April 21, 2017

# Abstract

Influenza virus is one of the most pervasive pathogenic threats to the global public health on an annual basis. Each year, this RNA virus causes hundreds of thousands of deaths and billions of dollars in economic damage. The influenza vaccine is a key contributor in the fight against influenza infection and is available in several formulations, including the Live Attenuated Influenza Vaccine (LAIV). Although LAIV was sequenced nearly 20 years ago, the role of some of its genomic mutations have yet to be characterized.

I believe the NS gene segment contributes to the attenuation phenotype of LAIV. To test this hypothesis, a panel of NS reassortant viruses in both the LAIV and A/Victoria/361/2011 backbones were generated. Additionally, a panel of recombinant viruses expressing a mutation at amino acid residue position 153 in the non-structural protein 1 (NS1) C-terminal domain were generated in both the LAIV and A/Victoria/361/2011 backbones. The NS reassortant viruses were generated, sequence verified, and characterized in MDCK and A549 cell culture systems. We show that a reassortant virus with LAIV NS in the A/Victoria/361/2011 backbone display faster growth kinetics in MDCK and A549 cell systems than its wild-type NS counterpart in the A/Victoria/361/2011 backbone. In MDCK cells, a reassortant virus with LAIV NS in the LAIV backbone displayed faster growth kinetics than a reassortant LAIV virus with wild-type NS. However, there was no significant difference in A549 cells. These data indicate the NS gene segment of influenza has a role in viral replication.

Primary Reader: Andrew Pekosz, Ph.D.

Secondary Reader: Jay Bream, Ph.D.

## Acknowledgement

I wanted to first thank my thesis advisor, Dr. Andy Pekosz for giving me the opportunity to work in his lab. Despite transferring into the ScM program late and having no experience in a biological lab, he lent me his time, expertise, and resources to further my academic career. I'm also in debt to members of the lab – Eddy Ye and Nick Wohlgemuth in particular for taking the time to train me. I also owe a good deal of gratitude to Dr. Katherine "Katie Bird" Fenstermacher for answering many of my questions, dealing with my countless sarcastic quips, and generally tolerating me over the course of a year. Many thanks are also in order for the other members of the Pekosz and Klein labs.

My parents also deserve recognition for having faith in my dream of becoming a physician, even as it dragged me halfway across the country. Their support has meant everything to me and I wouldn't have made it this far without them. I've had the privilege of becoming close friends with Brendan Dolan, Harrison Powell, and Payam Fathi, without whom I wouldn't have remained in MMI for another year. We found a common bond in our status as degenerate people who had similar interests in watching the Ravens lose on a Sunday afternoon, accidental trips to find buffalo wings, fresh creybs from the harbor, and roasting one another on a daily basis.

Finally, I wanted to thank the city of Baltimore. As a kid from the country, I was incredibly skeptical of moving into East Baltimore (so optimistically portrayed in The Wire), but the city grew on me. I soon found myself an O's fan who developed a taste for the fermented harbor water that they repackage as Natty Boh, and I was often rocked to sleep by the soothing sounds of ambulance and police sirens which served as my lullaby every night. And of course, I must appreciate my gratitude towards Buyo, our neighborhood cat who was also too excited to see me.

# Table of Contents

# Index of Tables

# Index of Figures

# Chapter 1 - Public Health Importance of Influenza

## 1.1 Influenza in the Population

### 1.1.1 History

Influenza has been a persistent threat to global public health for hundreds, if not thousands of years. Some of the earliest reports of influenza infections can be traced back to the Hellenic Era in Greece during the 5th century BC [1]. Historians suggest the first pandemic started in Asia in 1580 AD, spread to North Africa and Asia Minor into Europe [2]. In the span of six months, the pandemic had spread across the entirety of Europe and even to America. The ability for influenza to spread so readily is particularly impressive considering the lack of modern transportation like airplanes and motor vehicles. Nearly 10 other pandemics have been reported since 1580, the most notorious being the 1918 pandemic [1].

Although commonly referred to as the "Spanish Flu", the name of the 1918 pandemic is a bit of a misnomer. Some accounts attribute the source of the outbreak to Spain, others to America, and others still to China [1]. Modeling by Taubenberger and Morens estimated that "one third of the world's population (or ≈500 million persons) were infected and had clinically apparent illnesses . . .total deaths were estimated at ≈50 million and were arguably as high as 100 million" [3]. Hallmarks of the Spanish Flu included excessive morbidity in young adults (20-40 years old), a demographic that is historically quite resilient to influenza infections, and an increased susceptibility to secondary respiratory infections [4]. The pandemic of 1918 perfectly illustrates the volatile and dangerous nature of influenza. Antigenically similar strains of an influenza virus can be

transmitted regionally on a year-to-year basis and have a mild impact on mortality and morbidity, however, antigenically novel pandemic viruses can arise with little warning and devastate public health on a global level.

### 1.1.2 Classification and Diversity

Influenza is an RNA virus that belongs to the family *Orthomyxoviridae*. Influenza A, B, and C are capable of infecting humans, however Influenza A and B are of major concern for seasonal infection. Specific viruses are named in accordance with their influenza genera, location where strain was isolated, isolate number, and year isolated [5]. For example, A/Victoria/361/1972 was isolate number 361 of an influenza A virus isolated in Victoria, Australia during 1972. Influenza A viruses can be further classified by the antigenic properties of their hemagglutinin (HA) and neuraminidase (NA) surface glycoproteins [6]. To date, 18 HA and 9 NA subtypes have been identified and characterized. Of these HA and NA subtypes, only H1, H2, H3 and N1, N2 are known to maintain continued transmission within human populations.

### 1.1.3 Mortality and Morbidity

Influenza has a tangible and significant impact on public health in the US and abroad. Molinari et al. examined domestic influenza infections for 2003 and modeled its burden on patient health and financial toll on the healthcare system. Influenza infects around 25 million Americans each year, which results in 31 million outpatient visits to healthcare facilities [7]. Of these 31 million outpatient visits, up to 300,000 Americans are hospitalized each year as a result of influenza infection. Furthermore, around 30,000

patients will succumb to infection and die. It's very important to note that many of these fatalities are not directly attributable to the influenza virus, but rather opportunistic secondary infections that present in the days and weeks following influenza infection.

The Molinari et al. study also examined the financial burden of influenza in the US. Roughly $87 billion was spent in 2003 to treat influenza and its sequelae. The vast majority of these costs (83%) were attributable to the healthcare of patients who would eventually succumb to infection. When examining financial burden in regards to age strata, adults over the age of 65 accounted for over 60% of the total economic burden. In America, influenza primarily affects the elderly and older adults. Only 15% of total influenza expenditures can be attributed to people between the ages of 0-49.

### 1.1.4 High Risk Populations

The very young ($<$ 5 years of age) are at elevated risk of influenza when compared to adult populations. It should be noted that of total pediatric influenza-related fatalities in the US between 2004 and 2015, healthy children under the age of 5 without pre-disposing medical conditions accounted for roughly 50% of case fatalities [8]. Nearly half of these patients either died before being admitted to the hospital, had clinical illness for $<$ 3 days (typical infection lasts 7 days), or had secondary bacterial infection [8].

On the other end of the age spectrum, the elderly ($>$ 65 years of age) also bear a disproportionate amount of morbidity and mortality to influenza infection. Approximately 70-85% of seasonal influenza deaths and 55-70% of hospitalizations can be attributed to this age demographic [9]. Furthermore, when compared to the non-elderly, the elderly face a significantly greater risk of death (odds ratio = 2.95) in response to influenza infection [10].

There is also research to suggest that flu seasons in which H3N2 strains are predominant, the elderly face a much greater risk of influenza-related hospitalizations [11].

Exacerbation of pre-existing co-morbidities including Chronic Obstructive Pulmonary Disease (COPD), heart disease, and diabetes also significantly impacts a patient's health outcomes. The presence of any co-morbidity was associated with an increased risk of death (odds ratio = 2.04) [10]. These co-morbidities enhance the likelihood of hospitalization and the risk of developing pneumonia. When combined with pneumonia deaths, influenza was the #8 cause of death in the US in 2014[12].

Pregnant women are another group. During the 2009 pandemic H1N1 outbreak, when compared to their non-pregnant female counterparts, pregnant women exhibited higher rates of hospitalization, more admissions to the intensive care unit, and an increased likelihood of pre-term births and emergency cesarean sections [13]. It's believed that hormonal changes following conception disrupt inflammatory immune responses including natural killer cell activation, macrophages, and other Th1 response pathways that are crucial for combating diseases that are inflammatory, e.g. influenza [14].

The immunocompromised are at elevated risk of severe influenza infection [15]. These patients typically have a chronic infection like HIV, have undergone organ transplant, or are undergoing treatment for certain types of cancer. Unlike healthy individuals in the general populations, they are unable to mount T cell responses, are taking immunosuppressive drugs, or are receiving bone marrow transplants, respectively. These factors make it easier for them to contract, and more difficult to clear influenza infection. While, they are still advised to receive their annual flu shot, Kunisaki and Janoff identified that this group has dampened humoral immune responses following vaccination and thus vaccination may have reduced efficacy in this patient population [15].

The data presented thus far represents high-risk groups in developed nations, however, influenza also has a huge impact within the developing world. Nair et al. conducted a meta-analysis of 43 different studies that examined the mortality and morbidity of children within developing settings around the world. In 2008 alone, they estimated there were 90 million influenza infections in children under the age of 5, one third of which resulted in an influenza-related acute lower respiratory infection [16]. Of the roughly 30 million children who contracted a secondary infection, around 100,000 children died. The study found a 15-fold difference in case fatality ratio between developed and developing settings. Much of this can be attributed to a lack of resources and infrastructure needed to provide basic healthcare to patients. In stark contrast to developed countries that see the elderly as bearing the brunt of influenza morbidity and mortality, the very young are the most impacted by influenza infection in developing nations.

## *1.2. The Viral Lifecycle*

### 1.2.1 Genome Structure and Organization

Influenza has a negative sense, single-stranded RNA genome consisting of 8 unique gene segments. These gene segments are organized in order of decreasing gene segment size and each have a distinct role in the influenza life cycle:

| | Segment | Approx. Length (base pairs) | Protein Encoded and Function |
|---|---|---|---|
| 1 | PB2 | 2300 | PB2- RNA Polymerase subunit |
| 2 | PB1 | 2300 | PB1 - RNA Polymerase subunit |
| 3 | PA | 2200 | PA - RNA Polymerase subunit |
| 4 | HA | 1750 | HA - binding and membrane fusion |
| 5 | NP | 1550 | NP - structural nucleoprotein |
| 6 | NA | 1450 | NA - possesses a viral receptor destroying function necessary for vial release |
| 7 | M | 1000 | M1 and M2 - encodes matrix proteins |
| 8 | NS | 875 | NS1 - antagonization of host immune responses<br>NEP - viral RNP export from the nucleus |

Table 1. The Eight Gene Segments of the Influenza Virus

## 1.2.2 Virus Infection and Assembly

Mature influenza A and B virions can be either spherical or filamentous in shape and recognize host epithelial cells via sialic acid residues on their surface [5]. These sialic acid residues will either be in an α-2,3 or α-2,6- linkage conformation. HAs have different preferences for sialic acid linkage conformation, which help define host range and restriction. In the avian gut epithelium, α-2,3 linkages predominate, while the respiratory epithelium of humans varies based on location: the upper respiratory tract, the site of primary influenza infection, has mostly α-2,6 linkages, but α-2,3 linkages are more common in the lower lung [17,18]. Like humans, swine posses both sialic acid receptor linkages. Since HA is the primary glycoprotein responsible for host cell recognition, neutralizing antibodies are often directed to HA-specific epitopes. This places a selective

| | Segment | Approx. Length (base pairs) | Protein Encoded and Function |
|---|---|---|---|
| 1 | PB2 | 2300 | PB2- RNA Polymerase subunit |
| 2 | PB1 | 2300 | PB1 - RNA Polymerase subunit |
| 3 | PA | 2200 | PA - RNA Polymerase subunit |
| 4 | HA | 1750 | HA - binding and membrane fusion |
| 5 | NP | 1550 | NP - structural nucleoprotein |
| 6 | NA | 1450 | NA - possesses a viral receptor destroying function necessary for vial release |
| 7 | M | 1000 | M1 and M2 - encodes matrix proteins |
| 8 | NS | 875 | NS1 - antagonization of host immune responses<br>NEP - viral RNP export from the nucleus |

Table 1. The Eight Gene Segments of the Influenza Virus

## 1.2.2 Virus Infection and Assembly

Mature influenza A and B virions can be either spherical or filamentous in shape and recognize host epithelial cells via sialic acid residues on their surface [5]. These sialic acid residues will either be in an α-2,3 or α-2,6- linkage conformation. HAs have different preferences for sialic acid linkage conformation, which help define host range and restriction. In the avian gut epithelium, α-2,3 linkages predominate, while the respiratory epithelium of humans varies based on location: the upper respiratory tract, the site of primary influenza infection, has mostly α-2,6 linkages, but α-2,3 linkages are more common in the lower lung [17,18]. Like humans, swine posses both sialic acid receptor linkages. Since HA is the primary glycoprotein responsible for host cell recognition, neutralizing antibodies are often directed to HA-specific epitopes. This places a selective

pressure on the virus to develop slight mutations in HA such that the host must generate new memory cells directed against the drift HA. This subtle process of mutation is termed antigenic drift.

Following HA binding of sialic acid, the virion is endocytosed into the host cell. Acidification of the endosome triggers a conformational change in HA that merges the viral envelope with the endocytic membrane, forming a pore [19]. The influenza M2 protein then forms an ion channel for $H^+$ ions to be pumped into the viral particle. The further acidification denatures protein-protein interactions and allows freed viral RNPs to be exported into the host cytosol.

Once in the cytosol, nuclear localization signals on the viral RNPs communicate their transport into the host nucleus. One of these RNPs, the RNA-dependent RNA Polymerase, synthesizes mRNA templates for viral protein synthesis and a complimentary negative sense genome to be packaged into immature virions [20]. For proper maturation and export out of the nucleus, the PB1 subunit on the RNA Polymerase complex "snatches" 5'-guanosine caps from host pre-mRNA transcripts [21]. This has a dual effect to shut down host mRNA translation while allowing for maturation of viral mRNA. The poly-A tail of viral mRNAs is formed by encoding a series of 5-7 uracil residues on the negative sense script, which will then be transcribed into adenosine residues [22]. Once the 5'-end has been capped and 3'-tail polyadenylated, viral mRNAs are transported out of the nucleus using host mRNA machinery; M1 and NEP mediates this process by interacting with viral RNA and bringing them into contact with the RNP complex [20]. The viral genome assembles and is packaged into virions at the cellular membrane. Influenza virions bud from the cell membrane and the HA glycoprotein spikes continue to bind sialic acid residues on the cell surface. Viral release occurs when the NA protein utilizes its enzymatic

activity to cleave the sialic acid residue and release the influenza virion to infect other cells [23].

### 1.2.3 Symptoms and Transmission

Although pandemics are rare in occurrence, influenza is transmitted from individual to individual year-round across the globe. Of the three types of flu, only Types A and B contribute to seasonal epidemics[24]. The virus is spread through aerosolized droplets that are released as part of coughing and sneezing. These droplets contain infectious virions that infect nearby individuals either through inhalation or direct contact. Infection occurs in the epithelial cells of the upper respiratory tract of a host, and clinical symptoms can manifest as soon as 24 hours post infection with the appearance of a fever ($38^{o}$C - $40^{o}$C) [25].

Symptoms are commonly characterized by malaise, body aches, runny nose, dry cough, excessive sputum production, and other generalized respiratory symptoms (WHO, 2017). In healthy individuals with few pre-existing co-morbidities, symptoms typically resolve in one or two weeks[26]. However, those with chronic conditions are at greatest risk of fatal influenza infection, and may experience sequelae such as pneumonia that can complicate and prolong recovery[12]

There is a seasonality to influenza transmission (Figures 1 and 2). Generally speaking, the Northern Hemisphere experiences their peak transmission during the winter months - November through March. The Southern Hemisphere experiences their peak transmission during the late spring and summer months - April through August. The seasonality of influenza transmission in the tropics is much less defined, and outbreaks occur sporadically through the year.

**Number of specimens positive for influenza by subtype**
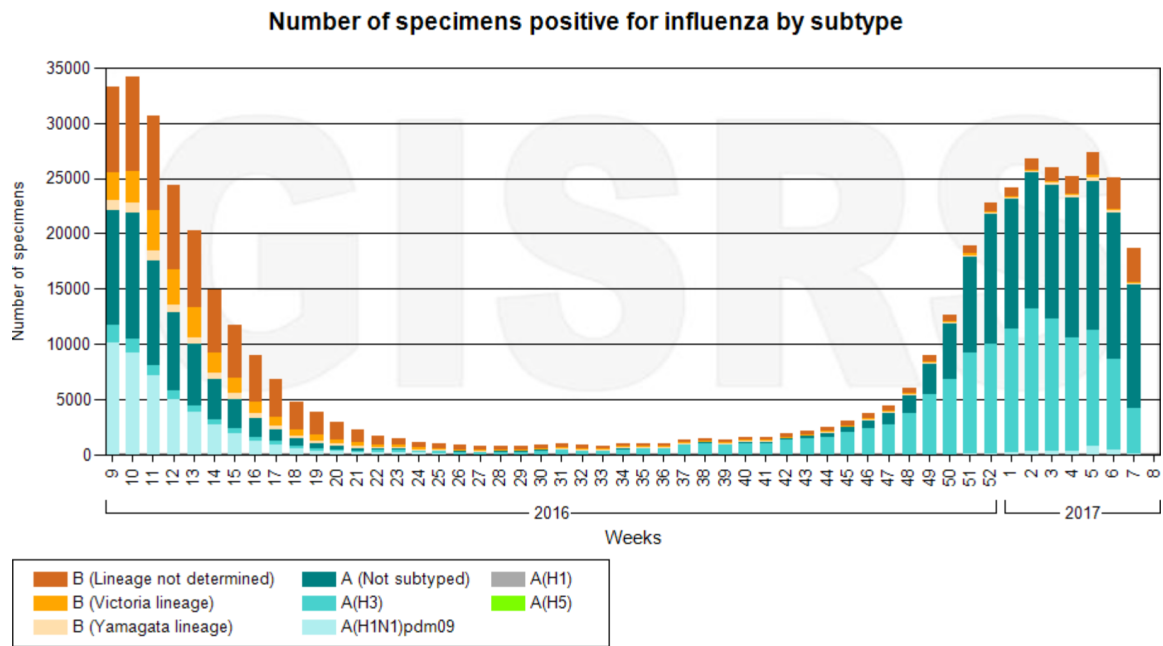


Figure 1. Positive Influenza Infection Tests in the Northern Hemisphere during 2016-2017. WHO, 2017

**Southern hemisphere**

**Number of specimens positive for influenza by subtype**



Figure 2. Positive Influenza Infection Tests in the Southern Hemisphere during 2016-2017. WHO, 2017

Unfortunately for epidemiologists and public health professionals, there is no discrete, singular reason why influenza infections peak during the winter months. One theory posits that serum levels of Vitamin D drop during this time as people are less likely to be outside[27]. Vitamin D has been connected to promoting mucosal and CD4+ T cell responses, so influenza may be able to infect hosts more readily as Vitamin D levels drop [28]. Some believe the seasonality of flu is related to social and behavioral factors including crowding which helps transmission by exposing more people to the aerosolized droplets of an infected individual [29]. A new theory suggests that the innate immune response is dampened by a drop in ambient temperature. Foxman et al. demonstrated that rhinovirus is able to infect humans more readily at 33° C due to diminished response by Type I interferons [30]. It would be particularly interesting to see if lowered ambient temperatures

enable influenza infection, or if viral proteins are better at inhibiting host immune responses at lower temperatures. A leading theory believes that a combination of temperature and humidity is the driving force in influenza seasonality. Guinea pigs held in cages at $5^{o}C$ and low humidity were much more prone to influenza infection than those held at $30^{o}C$ and normal/high humidity conditions [31]. Lowen and Steel attribute the higher infection rates to an increase in virion stability while aerosolized, however this is also highly dependent on the pH and salt balance of the droplets.

The underlying seasonality of influenza infection is far too complex to attribute to a single environmental or host immune factor. It's much more likely that a series of factors work in sync to increase infection rates during particular times of the year.


## 1.3 Influenza Vaccines

### 1.3.1 Vaccine Development

The manufacture of the influenza vaccine is a yearlong process that is coordinated through 80 different countries and requires a large amount of collaboration to ensure a viable vaccine is produced in sufficient quantity for distribution. Throughout the year, sentinel physicians send nasopharyngeal swabs from suspected influenza cases to WHO centers to sequence the HA and NA surface glycoproteins from the patients to monitor mutations that may change the antigenicity of either protein. Novel strains are sent to one of four influenza research centers for further molecular and genetic analyses [32]. The strains included in the annual influenza vaccine reflect the isolated strains obtained from yearlong surveillance. For countries in the Northern Hemisphere, circulating flu strains are reviewed in February to determine their potential for circulation during the next flu season.

The antigenic drift of existing vaccine strains is also evaluated in case a strain update needs to be made. Once the vaccine composition has been decided, vaccine companies have around 8 months to produce and release vaccines to health care providers [32].

In recent years, seasonal vaccines have included one H1N1, H3N2, and Influenza B strain which reflect the predominant circulating strains. Reassortant viruses are generated by growing the selected H1N1 and H3N2 strains in embryonated hen's eggs alongside an A/PR8/1934 strain which grows to high titer in eggs [33]. The surface proteins of progeny viruses are antigenically very similar to their wild type circulating precursors, but are still tested for their absence of genes coding for A/PR8/1934 surface glycoproteins. As part of the serial passage process, progeny viruses also develop mutations in order to propagate within eggs - these mutations must be tested to ensure they have not changed the antigenicity of the virus. There are no "master strains" for reassortant Influenza B viruses, so field isolates must be used.

The surface antigens of candidate strains are tested for their homology to the reference viruses and then sent to vaccine manufacturers to evaluate their potential for mass production. Strains that meet both of these criteria are selected for the annual vaccine. Vaccine strains are grown in the allantoic cavity of embryonated eggs, harvested, and inactivated by formalin or another similar agent. Next, the strains are partially purified by ultra-centrifugation and mild detergent disruption. After these steps, manufacturers must prove the purified strains have had no changes to the HA and NA genes. Finally, the antigen concentration of the purified viruses is quantified by an immune-diffusion assay.

In European countries, finalized vaccine candidates must undergo clinical studies to prove their safety and immunogenicity - this is not required in the United States.



**Flu vaccine production**

Developing a vaccine to combat the swine flu strain could take months, based on current production methods. For comparion, this is how the seasonal flu vaccine is made:

| Jan. | Feb. | March | April | May | June | July | August | Sept. | Oct. |
|------|------|-------|-------|-----|------|------|--------|-------|------|

- An FDA advisory panel selects three flu strains it believes will be circulating in the coming season.
  - The FDA distributes samples, or seed virus, of the strains to the manufacturers.
  - Seed virus is injected into chicken eggs. Each virus strain is made separately and later combined to make one vaccine.
- Millions of specially prepared eggs are used, each one is cleaned with a disinfectant spray and injected with one strain.
  - Virus multiplies in incubated eggs.
  - Virus is harvested.
- FDA tests for purity and potency of strains.
  - The strains are blended into one vaccine.
  - FDA licenses the vaccine.
- Vaccine is filled into vials and syringes, packaged. It is kept in cold storage.
- Vaccine is shipped.
- Vaccination begins; immunity develops about two weeks after getting the shot.

Sources: Aventis; Sanofi Pasteur; Centers for Disease Control and Prevention; USA TODAY research

By USA TODAY

Figure 3. Flu Vaccine Development Timeline for the Northern Hemisphere. USA Today, 2009

### 1.3.2 Vaccine Composition

There are two formulations for the annual vaccine. The most common is the injectable formulation that contains formalin-inactivated virions[34]. These virions have no ability to replicate within the host, but are capable of inducing a memory response by the immune system. The inactivated vaccine has greatest efficacy in patients above the age of 6 [35]. The increased efficacy in older children is most likely attributable to past infection with influenza virus.

The other formulation is a live attenuated influenza vaccine (LAIV) that is administered through a nasal spray into the nasopharyngeal region of the upper respiratory tract[36]. As the name implies, this is a live virus that can replicate within the host, but does not cause disease. This area of the body maintains a temperature around $32^{o}$C which permits localized viral growth, but prevents systemic infection into the lower airways which maintain a temperature around $37^{o}$C. LAIV is of note because its administration has been connected to a broad and systemic IgA mucosal response to not

only the vaccine strains, but also strains that have undergone genetic drift/shift [37]. The live

virus formulation is currently only recommended for people between the ages of 2-49 and

those who are not immunocompromised.

The inactivated and live attenuated formulations can be either trivalent or

quadrivalent. The trivalent vaccines have two influenza A strains and one influenza B

strain. The trivalent vaccine for the 2016-2017 season consisted of A/California/7/2009

(H1N1) pdm09-like, A/Hong Kong/4801/2014 (H3N2), and B/Brisbane/60/2008[34]. The

quadrivalent vaccines are identical to their trivalent counterparts except they contain a

second influenza B strain.

Growing vaccine strains in eggs has the disadvantages of scalability, potential for

undesirable mutations that decrease antigenicity of vaccine strains, contamination, and

constraints on egg availability, which has led to alternative means of production being

investigated. Cell lines may minimize some of these disadvantages, such as reducing the

risk of accidental mutations during the production process [38]. Furthermore, cells have the

advantage of being cryopreserved, stored, and scaled up if the need arises. Grown in

Madin-Darby Canine Kidney cells, FLUCELVAX® is the first cell-based vaccine to be

approved by the FDA and was first offered during the 2016-2017 flu season[39]. Clinical

studies indicated this vaccine induced immunogenicity to circulating influenza strains while

also demonstrating similar side effects to egg-derived vaccines [40].

Baculovirus expression vectors also represent a step forward in influenza vaccine

development. In this system, recombinant baculoviruses are engineered to encode a

cDNA for a foreign protein of interest [41]. These viruses then infect insect or plant cells,

producing the mRNA transcripts which can then be harvested and translated to the desired

protein. Flublok® is a novel vaccine though which recombinant influenza hemagglutinin is

produced, harvested, and purified into a vaccine formulation through these baculovirus

14

vectors. There are numerous advantages to baculovirus vectors when compared to eggs for vaccine production. One of the greatest benefits of this system is its safety. Baculoviruses are present on nearly every type of leafy green vegetable (and are ingested on a daily basis by humans) and are only known to infect moths and butterflies. Furthermore, much like cell culture systems, baculovirus systems are very scalable and take less time to clone, express, and manufacture the recombinant HA [42].

## 1.4 Non-Structural Protein 1

### 1.4.1 Protein Overview

The NS gene of influenza viruses encodes two separate proteins, non-structural protein 1 (NS1) and nuclear export protein (NEP). Both of these proteins are produced during an infection, but are not packaged into progeny virions. The NS1 protein is a multifunctional protein, however its overall role in antagonizing innate immune responses can be connected to one of its two functional domains. The first is the N-terminal domain,

also known as the RNA-binding domain, and then the C-terminal domain, also known as the effector domain [43].



Figure. 4. Structure of the NS1 Protein and Cellular Targets of Immune Inhibition. Hale et al., 2005

### 1.4.2 Structure and Function of the N-terminal Domain

The N-terminal domain is roughly defined as amino acids 1-73 of the NS1 protein. As mentioned previously, the N-terminal domain of NS1 is responsible for directly binding host RNA and preventing its transcription into proteins. The N-terminal domain forms a homodimer in solution that consists of three α-helical domains which constitute the majority of secondary structure for this region of the protein. This dimerization is crucial for RNA binding. The α-helices of the homodimer form a unique chain fold that binds RNA between the 2 and 2' chains [43]. Research has determined that within the second α-helix, R38 and K41 are the two crucial amino acids needed for RNA-binding [44]

The NS1 N-terminal domain is well-known for inhibiting the 2'-5' oligoadenylate synthetase (OAS)/RNAse L pathway. The OAS/RNAse L pathway is activated by IL-1β, a

key cytokine in initiating a wide array of innate immune responses, and is known to induce an antiviral response by recognizing and degrading foreign dsRNA [45]. It was originally thought that NS1 inhibited production of IL-1β which would block OAS/RNAse L. However, work conducted by Min and Krug found that NS1 functions not to prevent the transcription of IL-1β, but rather to directly bind viral dsRNA and sequester it from the OAS recognition complex and thus prevent its degradation via RNAse L [46]. Furthermore, Min and Krug found that an R38A mutation in the N-terminal domain effectively abolished NS1 inhibition of the OAS/RNAse L pathway. This discovery implicates point mutations as key mediator of NS1 antagonism of the innate immune system.

The N-terminal domain has also been proven to directly inhibit the production of key innate cytokines including IL-1β and IL-18. Stasakova et al. utilized A/Puerto Rico/1934 viruses with nucleotide base deletions in the C-terminal of the NS1 protein. The levels of IL-1β and IL-18 in the truncated NS1 mutant viruses were found to be similar to that of the full-length A/Puerto Rico virus [47]. Furthermore, mutant viruses expressing an impaired N-terminal domain resulted in IL-1β levels that were 10-50 times higher, and IL-18 levels that were five times higher than the full length virus. These data implicate the N-terminal domain of NS1 in IL-1β and IL-18 inhibition.

### 1.4.3 Structure and Function of the Linker Region

There is a short linker region of roughly 11 amino acids that separates the N-terminal and C-terminal domains. The length of the linker region is strain dependent and is believed to give NS1 a certain degree of flexibility with the C-terminal rearranging itself around a stationary N-terminus [48]. This will influence the three-dimensional structure of the protein and potentially alter its interaction with other cellular factors. Truncated linker

regions have been connected to an increase in virulence in some H5N1 viruses, suggesting its potential importance in modulating NS1 function [49].

### 1.4.4 Structure and Function of the C-terminal Domain

The C-terminal domain of NS1 is characterized as extending from amino acids 85 to the end of the protein; the exact length of the C-terminus is strain-dependent. Although the N-terminus remains dimeric throughout the course of infection, the C-terminus is capable of forming dimers or remaining monomeric [48]. Since both functional domains of NS1 act as dimers, researchers now believe the protein acts as a dimer *in vivo* [50]. However, NS1 can cycle between monomeric and dimeric conformations to determine which is most beneficial at that point of the infection. For example, the protein may be monomeric during early infection when the protein concentration is low, but may then cycle to an open dimer during later stages when the protein concentration has increased and can bind host factors like CPSF30. These structures can be further influenced in a strain-dependent manner. The tertiary structure of the C-terminal domain, as well as the N-terminal domain is fairly conserved across influenza strains. However, the effector domain is known to display polymorphisms that influence its interaction with host mRNA transcripts and cellular factors. Carrillo et al. determined there are three main classes of NS1 effector domain orientation: open, semi-open, and closed [48]. Furthermore, there is evidence to suggest that these orientations are influenced by linker region length and residue composition. This flexibility may allow for varying conformations in quaternary structure that would influence NS1's interactions with host factors and result in the protein's known multi-functionality [51].

The C-terminal domain of NS1 is multifunctional and works to inhibit host cell innate immune responses to various degrees.

One of the most studied targets of NS1's C-terminal domain is cleavage specific polyadenylation factor (CPSF30). CPSF30 is responsible for the maturation of host pre-mRNA by cleaving the 3'-end of the transcript and then polyadenylating the end of the cleavage site [52]. This process is critical for proper development of host mRNA such that it can be exported from the nucleus. NS1 functions to bind and sequester CPSF30 so it cannot complete this function. The result is a bottleneck on the export of host mRNA, most notably mRNA encoding Type I interferons. As the host mRNA accumulates, the viral replication complex binds host transcripts via the PB2 subunit, cleaves the transcripts via the PA subunit, and finally prepares viral mRNA synthesis with the PB1 subunit [53]. It's necessary to note that these viral RNA transcripts can be transcribed independently of host machinery and are thus selectively omitted from this block on transcription.

Discrete amino acids are crucial for the bioactivity of the NS1 effector domain. Work conducted by Twu et al. demonstrated that viruses with mutations at residues 144 and/or 186 in their NS1 C-terminus had 40 times more IFN-β than their wild type counterpart [54]. These researchers also implicated the a.a. 144-186 region as the binding site for the F2F3 zinc finger on CPSF30 [54]. These findings were built upon by Das et al. who demonstrated that amino acids F103 and M106 were crucial to maintain the stability of the NS1-CPSF30 complex [55]. These residues were highly conserved across > 99% of Influenza A strains and present an interesting target for anti-viral drug design in the future These data further reinforce the belief that point mutations in the NS1 protein can drastically influence the attenuation of influenza A viruses. It is also necessary to note that circulating seasonal influenza viruses show a strong capability to bind CPSF30, while egg adapted strains lack this trait [56]. Further work needs to be conducted to determine if egg

adapted strains attribute their adaptation specifically to inability to bind and inactivate CPSF30.

PABPII works in conjunction with the CPSF30 complex. CPSF30 cleaves the 3'-end of the pre-mRNA transcripts while PABPII ligates the complex following cleavage. Unsurprisingly, NS1 targets PABPII in addition to CPSF30. NS1 inhibition of PABPII is also believed to affect export of mRNAs. The PABPII complex is known to shuttle between the nucleus and cytoplasm and it has been hypothesized it may play a role in both the maturation and delivery of host mRNAs. Li et al. demonstrated that cells transfected with NS1 have sequestered and relocalized PABPII in the nucleus where it cannot interact with host mRNA [57]. Furthermore, the NS1 C-terminal domain appears to have non-overlapping regions that bind CPSF30 and PABPII - this means one protein can effectively bind and neutralize two host transcription factors. CPSF30 and PABPII also bind each other *in vitro* and form a complex. These data suggest that although CPSF30 may be able to bind host pre-mRNAs during an influenza infection, the conjoined binding with PABPII on the NS1 protein may still inhibit the proper maturation of host transcripts. Once again, point mutations in the aa 223-237 were implicated in NS1 binding on PABPII.

Protein kinase R is an intracellular sensor for dsRNA and serves as an important part of the innate immune system. Once activated by dsRNA, PKR phosphorylates the eIF2 translation factor which in turn halts host protein synthesis for both normal host function and viral invaders [58]. Influenza counteracts this in two ways. The first is inhibition of p58IPK, a factor that is required to activate PKR [59]. Secondly and more important for this research, is inhibition of PKR by NS1. NS1 binds amino acids 123-127 in the C-terminal domain and is believed to trigger a conformational change in PKR [60,61]. This conformational change prevents PKR from binding viral dsRNA and thus inhibiting its

translation. Once more, point mutations are implicated in maintenance of pro-viral functions in the host.

## 1.5 The Live Attenuated Influenza Virus

### 1.5.1 Overview and Description

The live attenuated influenza virus (LAIV) was developed concurrently in the US and USSR during the 1960s. The A/Ann Arbor/6/60 (US) and A/Leningrad/134/47/57 (USSR) wild type strains are both H2N2 viruses that were serially passaged at progressively lower temperatures in embryonated hens eggs [62]. As part of the serial passaging process, the wild type strains developed a set of mutations in its genome that allowed for its propagation under these conditions. The result was an antigenically distinct cold adapted (ca) progeny strain of the clinically isolated wt A/Ann Arbor/6/60. Genomic analyses have connected these mutations to three main phenotypes of LAIV that contribute to its attenuation.

1) Cold Adaptation - LAIV can propagate at $25^{o}C$. This is considerably lower than the core human body temperature of $37^{o}C$.

2) Temperature Sensitivity - LAIV has diminished replication efficiency at $37^{o}C$. LAIV is delivered into the nasopharyngeal tract via intranasal administration where the virus can replicate at $32^{o}C$. Although the upper airways permit a small, localized infection, the temperature sensitivity of the virus prevents it from spreading into the lower airways (temp. $\approx 37^{o}C$) which is associated with a more severe infection.

21

Instead, the virus remains localized to the upper airways where it can be controlled by the immune response.

3) Attenuation - Ferrets represent an animal model of influenza infection [63]. It has been shown that LAIV infection in these mammals limits influenza infection to the upper airways, but still induces a protective antibody response [64]. Furthermore, histological analyses of ferrets infected with LAIV demonstrated fewer lesions than those who were inoculated with the wild-type strains.

**1.5.2 LAIV Formulation**

In terms of an annual influenza vaccine, reverse genetics are used to create an LAIV through a 6:2 reassortment with the circulating wt virus of concern. The allantoic cavity of an embryonated hen's egg is infected with a cold adapted influenza strain like A/Ann Arbor/6/60 and the circulating strain of choice. In the egg, the six internal gene segments (PB2, PB1, PA, NP, M, NS) of the cold adapted strain reassort with the HA and NA from the circulating strain [65]. The resulting virus inherits the temperature sensitivity and attenuation of the cold adapted virus, but contains the external genes of the circulating strains that are necessary for generating an immune response.

Figure 5. Formulation of LAIV. Modified from NIAID.

### 1.5.3 NS1 Mutations in LAIV

It's clear that point mutations are responsible for the attenuation and temperature restriction of LAIV. Most of the mutations occur in the genes encoding viral polymerases, however a few have been discovered elsewhere in the genome, notably in the NS gene.

Work conducted by Cox et al. mapped one mutation in the coding region of the NS gene segment. Occurring at amino acid 153, the mutation from an alanine (wt) to a threonine (LAIV) was the only difference in the coding region of the NS gene of cold adapted A/Ann Arbor/6/60 when compared to the wt [66]. When examined in the same context as some of the other gene segments, it's reasonable to infer that the mutation at aa 153 of NS might have a role in LAIV attenuation.

| Segment | Coding Changes | Mutation | Effect |
|---------|----------------|----------|--------|
| PB2 | 1 | N265S | Attenuation, Temp. Sensitivity |
| PB1 | 4 | K391E, E457D, E581G, A661T | Attenuation, Temp. Sensitivity |
| PA | 2 | K613E, L715P | Cold Adaptation, Attenuation |
| NP | 2 | T23N, A34G | ? |
| M | 1 | A86S | Attenuation |
| NS | 1 | A153T | ? |

Table 2. Mutations in A/Ann Arbor/6/60 Arising During the Serial Passage and Cold Adaptation Process

### 1.5.4 Previous Data

Work conducted by Fenstermacher and Forero examined the growth kinetics of HA/NA-antigenically matched LAIV and wt A/Victoria/361/2011 in cultures of human nasal epithelial cells (hNECs) at 33$^{o}$C. They found that over a seven day period, infectious particle production as well as growth rate in LAIV was less than its wt counterpart [67].

In addition to altered growth kinetics, LAIV differentially induces the host innate immune response when compared to a wt virus. When hNEC cells were infected at a high multiplicity of infection (MOI), LAIV induced a larger number of genes distinct from the wt virus.

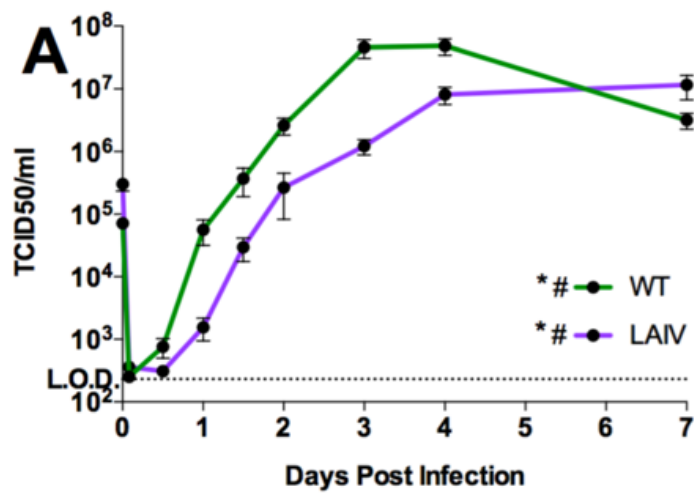Figure 6. LAIV Demonstrates Altered Growth Kinetics when Compared to wt A/Victoria/361/2011. Forero and Fenstermacher et al., ahead of print.
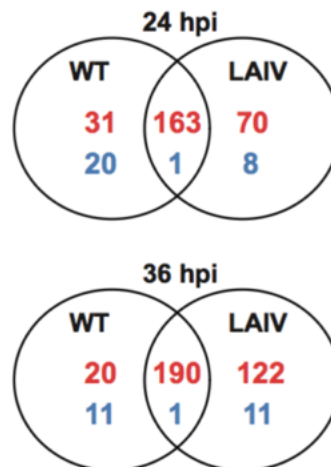


Figure 7. LAIV Differentially Induces the Immune Response. Forero and Fenstermacher et al., ahead of print.

At 24 hours post infection, LAIV induces over twice the amount of unique genes when compared to the wt. Furthermore, at 36 hours post infection, LAIV induces six times

the amount of genes distinct from wt. These data indicate LAIV and circulating wt viruses

differ in both replication and induction of the immune response, however the mechanistic

basis of these differences remains to be fully understood.

Previous work indicates that discrete amino acids are crucial for NS1's bioactivity.

Recent work conducted by Nogales et al. demonstrated that D189N and V194I mutations

in clinical isolates contributed to viral attenuation and temperature sensitivity, particularly

at aa 194 (Nogales et al., 2016). Furthermore, DeDiego et al. has shown that H3N2 viruses

bearing an I64T mutation are particularly susceptible to IFN-based responses [68].

In the context of these data, we believe the aa 153 mutation in the NS segment

may contribute to the attenuation of LAIV by participating in restricting viral growth and/or

differentially inducing immune genes distinct from wt influenza infection.


# Chapter 2 - NS Segment Reassortant Viruses between wild-type influenza A virus and live attenuated influenza virus vaccine

## *2.1 Introduction*

### 2.1.1 Influenza and Gene Reassortment

Reassortment of the influenza genome is a normal part of the virus lifecycle in

which entire gene segments are replaced by those of another influenza strain. This often

occurs in an intermediary species, swine for example, where avian and human influenza

viruses can co-mingle within the same pig [69]. For example, a human influenza can some

of its gene segments with that of an avian strain. The resulting reassorted virus has traits

of both its parental viruses which can have a profound impact on virulence within a naive host.

This process of reassortment is commonly known as genetic shift when it involves the HA gene segment and is a hallmark of influenza diversity and adaptation. Many pandemic strains have formed as a result of gene reassortment including the 1918 H1N1, 1957 H2N2, 1968 H3N2, and most recently 2009 H1N1 outbreak. A closer look at the 1918 pandemic strain shows the acquisition of an avian HA gene which drastically enhanced virulence when compared to its original lineage (Pappas et al. 2007).



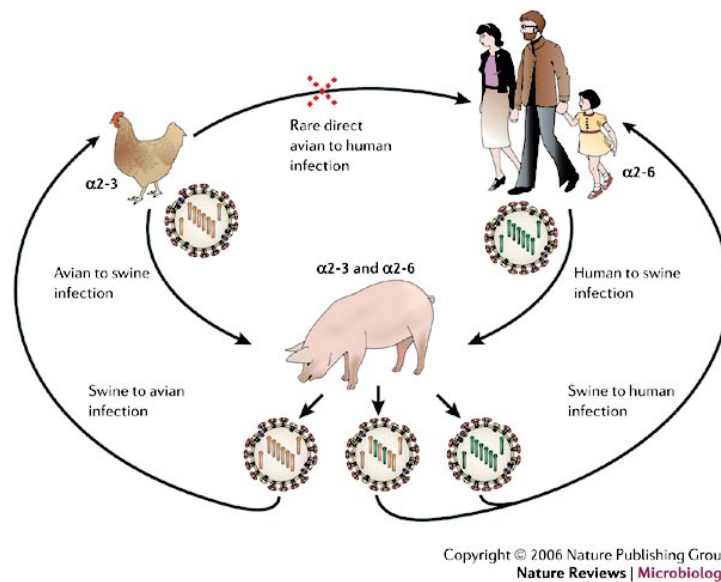Figure 8. Hypothetical Reassortment of Influenza within a Swine Host. Stevens et al., 2006.

**2.1.2 Reassortant Viruses in the Laboratory**

In the laboratory, we are able to manually induce gene reassortment to create new influenza viruses. In fact, this is done on an annual basis with LAIV which contains the six internal cold adapted genes from the attenuated virus, as well as the two external genes

27

from the circulating virus subtypes. When a single segment is substituted for another, the resulting virus is referred to as a "7:1 virus" to represent the seven original segments and the one transplant segment. These reassortant viruses are useful in determining the influence of a particular segment on viral phenotype. For example, the aforementioned work conducted by Pappas et al. was done with reassorted H1N1 viruses to elucidate that HA was the crucial segment conferring enhanced virulence in the 1918 pandemic strain. For the purposes of this project, we intend to do NS gene swaps between LAIV and wt A/Victoria/361/2011.

| | Lineage of Segments 1-7 | Lineage of NS Segment | Abbreviation |
|---|---|---|---|
| 1 | A/Victoria/361/2011 | A/Victoria/361/2011 | WT/WT |
| 2 | A/Victoria/361/2011 | LAIV | WT/LAIV |
| 3 | LAIV | LAIV | LAIV/LAIV |
| 4 | LAIV | A/Victoria/361/2011 | LAIV/WT |

Table 3. 7:1 Virus Panel



Figure 9. Representation of 7:1 NS Gene Swaps between wt A/Victoria/361/2011 and LAIV

Since the NS segment encodes two proteins, NS1 and NEP, sequence alignments of wild type A/Victoria/361/2011 and LAIV NS1 and NEP were performed in order to examine amino acid differences. There are 28 discrete amino acid differences between the wild type and LAIV NS1 proteins. In regards to NEP, there are 7 discrete amino acid differences. When used in our NS reassortant virus system, this variation in amino acids between the protein sequences might shed light on LAIV attenuation.



Figure 10. Sequence Alignment of wild type A/Victoria/361/2011 and LAIV NS1



Figure 11. Sequence Alignment of wild type A/Victoria/361/2011 and LAIV NEP

## 2.2 Materials and Methods

### 2.2.1 Cell Lines

Madin-Darby canine kidney (MDCK) cells were maintained in Dulbecco's Modified Eagle's Medium (DMEM) with 10% fetal bovine serum (FBS), 100 U/mL penicillin, 100 ug/mL streptomycin and 2mM L-glutamine at $37^{o}$C with 5% $CO_2$ and passaged at a 1:10 dilution every 3-4 days.

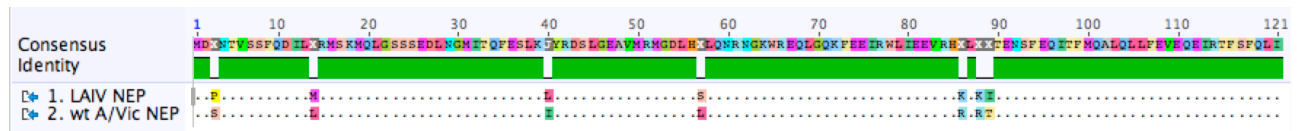Transformed human embryonic kidney 293 cells (293T) were maintained in DMEM with 10% fetal bovine serum (FBS), 100 U/mL penicillin, 100 ug/mL streptomycin and 2mM L-glutamine at $37^{o}$C with 5% $CO_2$ and passaged at a 1:10 dilution every 3-4 days.

Adenocarcinomic human alveolar basal cells (A549) were maintained in DMEM with 10% fetal bovine serum (FBS), 100 U/mL penicillin, and100 ug/mL streptomycin at $37^{o}$C with 5% $CO_2$ and passaged at a 1:10 dilution every 3-4 days.

### 2.2.2. Recombinant Viruses

A 12 plasmid recombinant virus rescue system was utilized to generate the panel of reassortant viruses (Neumann et al., 1999). 6-well plates were coated with poly-L-lysine and 293T cells were plated at 40-60% confluence 24 hours prior to transfection. For the reassortant viruses with the A/Victoria/361/2011 genome, 293T cells were transfected with A/Victoria/361/2011 pHH21 plasmids encoding the A/Vic PB2, PB1, PA, NP, NA, HA, M (0.5 µg each) and the LAIV NS segment (1.0 µg). For reassortant viruses with the LAIV genome, 293T cells were transfected with LAIV pHH21 plasmids encoding PB2, PB1, PA, NP, NA, HA, M (0.5 µg each) and the A/Vic segments HA, NA, and NS (1.0 µg). All pHH21 plasmids were transfected with helper plasmids encoding the ORFs of the A/Udorn/72 PB1, PB2, NP (1.0 ug each) and PA (0.2 uh) under the control of RNA polymerase II promoters which allows for expression of the viral proteins needed for RNA replication.

Transfection reagent TransIT-LT-1 (LT1) (Mirus) (20 µL/transfection) was mixed with OptiMEM medium (Gibco) (100 µL/transfection) and incubated at room temperature for 15 minutes. Plasmids were mixed at the aforementioned quantities, added to the LT1/OptiMEM mixture, and incubated at room temperature for another 15 minutes. DMEM was aspirated from 6-well plates containing 293T cells and replaced with 2 mL/well of

OptiMEM. The corresponding transfection mix was added dropwise to each well. The plates were incubated at $32^{o}C$ with 5% $CO_2$. 24 hours following transfection, 2.24 µL of 5 µg/mL N-acetyl trypsin (NAT) (Sigma) was added to each well to bring the total concentration of NAT to 10 µg/mL. The cells were incubated at $32^{o}C$ with 5% $CO_2$ for 4 hours and then each well overlaid with approx. $5*10^{5}$ MDCK cells suspended in 100 µL OptiMEM. The plates were transferred to a $37^{o}C$ incubator. Every 24 hours for approx. five days, 1 mL of supernatant was removed from the cells and replaced with 1 mL DMEM with 4 µg/mL NAT, 100 U/mL penicillin, 100 µg/mL streptomycin, 2mM L-glutamine, and 0.5% bovine serum albumin (BSA) (Sigma) (IM+NAT). Transfection was discontinued when indications of comprehensive cytopathic effects were observed.

WT/WT, WT/LAIV, LAIV/LAIV, and LAIV/WT reassortant viruses were generated in accordance with this protocol.

### 2.2.3 $TCID_{50}$ Assay

Fifty percent tissue culture infectious dose ($TCID_{50}$) were utilized to determine viral titers. MDCK cells were plated to confluence in 96-well plates. Viral supernatants were diluted at concentrations from $10^{-1}$ to $10^{-8}$ in IM+NAT. 20 µL of each 10-fold dilution was added to six consecutive wells on a confluent 96-well plate containing MDCK cells. These plates were incubated at $32^{o}C$ with 5% $CO_2$ for 7 days. The cells were fixed with 4% formaldehyde and stained with naphthol blue-black overnight. Cytopathic effects (CPE) were scored visually and $TCID_{50}$ was quantified using the Reed and Muench calculation.

### 2.2.4 Plaque Purification

Recombinant influenza viruses generated following transfection must be purified from the transfection supernatant. 6-well plates were seeded with MDCK cells and seeded to confluence. 100 µL of transfection supernatant was serially diluted ten-fold from $10^{-1}$ to $10^{-8}$ with IM+NAT. 6-well plates were aspirated and washed twice with PBS+. 250 µL of diluted virus (dilutions determined from $TCID_{50}$ of transfection supernatant) was added to each well. The 6-well plates were incubated for one hour at $32^{o}C$ for the LAIV/LAIV and LAIV/WT viruses and $37^{o}C$ for the WT/WT and WT/LAIV viruses. During the incubation period, the plates were gently tapped every 15 minutes to evenly distribute virus. Following incubation, the inoculum was aspirated and replaced with ~ 4 mL of a mixture of 2% agarose, 2X Modified Eagle's Medium (MEM), and 4 µg/mL NAT. Plates were incubated at $32^{o}C$ for 72-120 hours. Clear, defined, and singular plaques were picked using a 1 mL serological pipette, placed into tubes containing 500 µL IM, and stored at $-80^{o}C$.

### 2.2.5 Virus Infection to Generate Viral Stocks

MDCK cells were grown to confluence in T150 ($150 \text{ cm}^2$) flasks. 100 µL of the media containing the plaque plug was added to 5 mL IM+NAT. The media was aspirated from the T150 flasks and replaced by the virus and IM mixture. The flasks were incubated for one hour at $32^{o}C$ for viruses with LAIV polymerase genes and $37^{o}C$ for viruses with A/Victoria/361/2011 polymerase genes. During the incubation period, the plates were gently tapped every 15 minutes to evenly distribute virus. Following the one hour incubation, the inoculum was aspirated and replaced with 20 mL IM. The cells were monitored daily for CPE and the supernatants harvested after 30-40% of cells were dead or had detached from the flask. The infected cell supernatants were aliquoted into 200 µL volumes and stored at $-70^{o}C$ to establish a bank of viral seed stocks. The seed stocks

were sequenced to confirm a purified virus product and later infectious virus titers determined via $TCID_{50}$ assay. Once viral sequencing was completed, working stocks were generated from the seed stocks (MOI = 0.001) in the manner described above. Working stocks were also titrated for infectious virus via $TCID_{50}$ assay.

### 2.2.6 Low MOI Growth Curves

Growth curves were implemented to examine virus replication kinetics and peak viral titers mimicking natural infection. 24-well plates were seeded to confluence with either MDCK or A549 cells. Viruses were diluted to a multiplicity of infection (MOI) of 0.01 infectious viral particles per cell in IM+NAT. The NAT was added at a 1:1000 dilution for MDCK cells and 1:5000 dilution for A549 cells. The media was aspirated from the 24-well plates and each well was washed twice with PBS+. 250 µL of virus was added to appropriately labeled wells and incubated for one hour at $32^{o}C$ or $37^{o}C$. The viral inoculum was removed after the one hour incubation, the cells were washed twice with PBS+, and 500 µL IM+NAT added to each well. The IM+NAT was removed, stored, and replaced with fresh media at 1, 12, 24, 36, 48, and subsequent 24 hour time points until the cells has comprehensive CPE. The infectious virus titers were determined via $TCID_{50}$ assay. Virus particle production was graphed using Prism 7 software.

### 2.2.7 High MOI Growth Curves

Growth curves were implemented to examine virus replication kinetics and peak viral titers. 24-well plates were seeded to confluence with A549 cells. Viruses were diluted to a multiplicity of infection (MOI) of 0.55 infectious viral particles per cell in IM+NAT. The

media was aspirated from the 24-well plates and each well was washed twice with PBS+. 250 µL of virus was added to appropriately labeled wells and incubated for one hour at $32^oC$ and $37^oC$. The viral inoculum was removed after the one hour incubation, the cells were washed three times with PBS+, and 500 µL  IM+NAT added to each well. The IM+NAT was removed, stored, and replaced with fresh media at 1, 12, 18, 24, 36, 48, and subsequent 24 hour time points until the cells had comprehensive CPE. The collected supernatant was titered via $TCID_{50}$ assay. Virus particle production was graphed using Prism 7 software.

## *2.3 Results*

### 2.3.1 Rescue of NS Reassortant Viruses

 NS reassortant viruses were successfully rescued. All eight gene segments were sequenced to ensure there were no incidental mutations that occurred during the transfection process.

### 2.3.2 Replication of NS Reassortant Viruses at $32^oC$ in MDCK Cells

To characterize replication kinetics and peak viral titers of NS reassortant viruses, a multi-step growth curve was performed on MDCK cells at $32^oC$. This temperature was selected in order to mimic the temperature of the upper respiratory tract. When matched for genetic backbone, the LAIV/LAIV virus had significantly faster replication kinetics than the LAIV/WT virus, however they both reached the same peak titer at 72 hours post infection (Fig. 12). The WT/LAIV virus also had significantly faster replication kinetics than

34

the WT/WT virus, however both reached roughly the same peak titer at 72 hours post infection (Fig. 13).



Figure 12. Effect of NS Gene Swap in the LAIV backbone at 32°C in MDCK Cells. A multistep growth curve was performed on MDCK cells with the indicated viruses. Statistical differences were determined by MANOVA followed by Bonferroni post-test. *=P < 0.05; **= P < 0.01; ***=P<0.001. L.O.D=limit of detection=2.37.

**32C - WT/LAIV vs WT/WT**

Figure 13. Effect of NS Gene Swap in the A/Victoria/361/2011 backbone at 32$^{o}$C in MDCK Cells. A multistep growth curve was performed on MDCK cells with the indicated viruses. Statistical differences were determined by MANOVA followed by Bonferroni post-test. *=P < 0.05; **= P < 0.01; ***=P<0.001. L.O.D=limit of detection=2.37.

## 2.3.3 Replication of NS Reassortant Viruses at 37$^{o}$C in MDCK Cells

A multistep growth curve was also performed at 37$^{o}$C to mimic an infection of the lower respiratory tract, which is also representative of core body temperature. Once again, the LAIV/LAIV virus had significantly faster replication kinetics than LAIV/WT, but both viruses achieved roughly the same peak titer at 48 hours post infection (Fig. 14). Additionally, the WT/LAIV virus had significantly faster replication kinetics than the WT/WT virus, however both strains reached roughly the same peak titer at 48 hours post infection (Fig. 15).
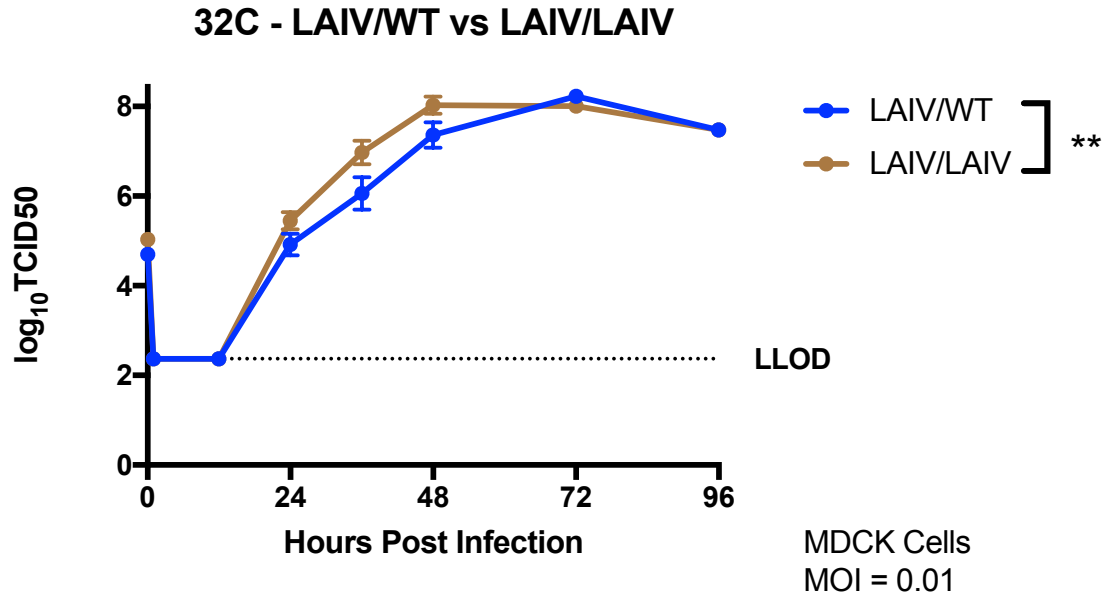
**37C - LAIV/WT vs LAIV/LAIV**

Figure 14. Effect of NS Gene Swap in the LAIV backbone at 37°C in MDCK Cells. A multistep growth curve was performed on MDCK cells with the indicated viruses. Statistical differences were determined by MANOVA followed by Bonferroni post-test. *=P < 0.05; **= P < 0.01; ***=P<0.001. L.O.D=limit of detection=2.37.

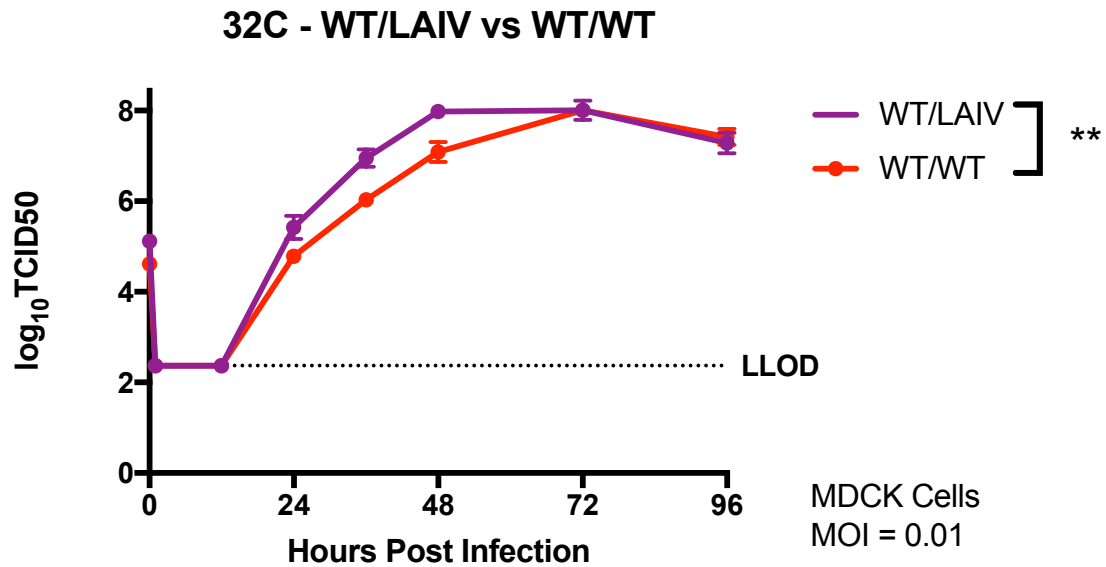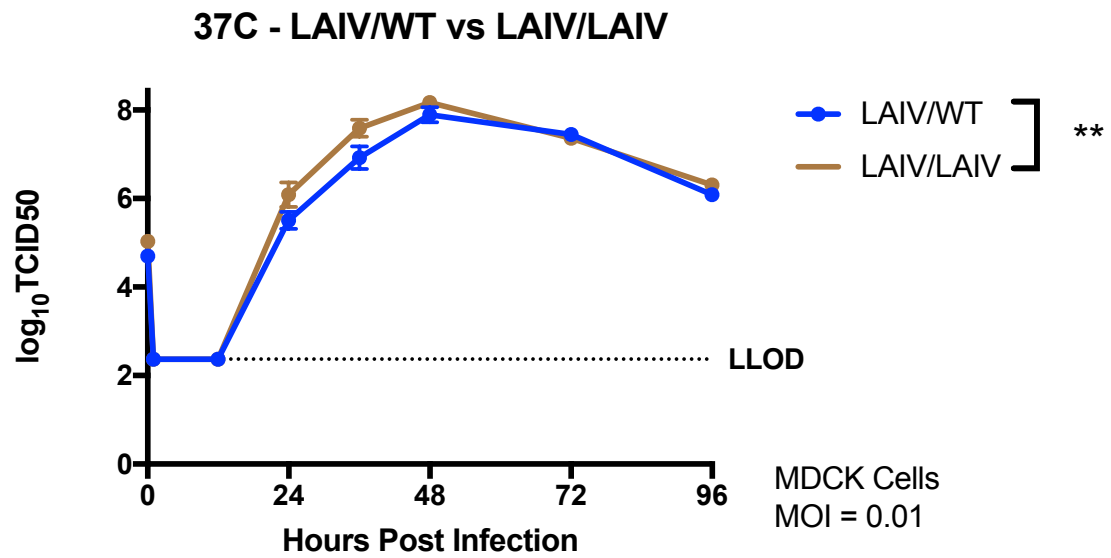**37C - WT/LAIV vs WT/WT**

Figure 15. Effect of NS Gene Swap in the A/Victoria/361/2011 backbone at $37^{o}$C in MDCK Cells. A multistep growth curve was performed on MDCK cells with the indicated viruses. Statistical differences were determined by MANOVA followed by Bonferroni post-test. *=P < 0.05; **= P < 0.01; ***=P<0.001. L.O.D=limit of detection=2.37.

## 2.3.4 Replication of NS Reassortant Viruses at $32^{o}$C in A549 Cells

A549 cells were infected to further evaluate viral growth kinetics for the NS reassortant viruses. Originating from adenocarcinomic alveolar basal epithelial cells, A549s present a more humanized model for influenza infection than MDCK cells. The A549 cells were infected at an MOI = 0.55.

A multistep growth curve was performed at $32^{o}$C. For the viruses in the LAIV backbone, the LAIV/LAIV and LAIV/WT viruses show no significant difference in replication kinetics – both viruses reached roughly the same peak titer at a similar rate (Fig. 16). For the viruses in the A/Victoria/361/2011 backbone, the WT/LAIV virus reached a peak titer nearly 100-fold greater than its WT/WT counterpart. Furthermore, the WT/LAIV virus reached its peak titer at a faster rate than the WT/WT virus (Fig. 17).

38

**32C - LAIV/WT vs LAIV/LAIV**

Figure 16. Effect of NS Gene Swap in the LAIV backbone at $32^{o}$C in A549 Cells. A multistep growth curve was performed on MDCK cells with the indicated viruses. Statistical differences were determined by MANOVA followed by Bonferroni post-test. *=P < 0.05; **= P < 0.01; ***=P<0.001. L.O.D=limit of detection=2.37.
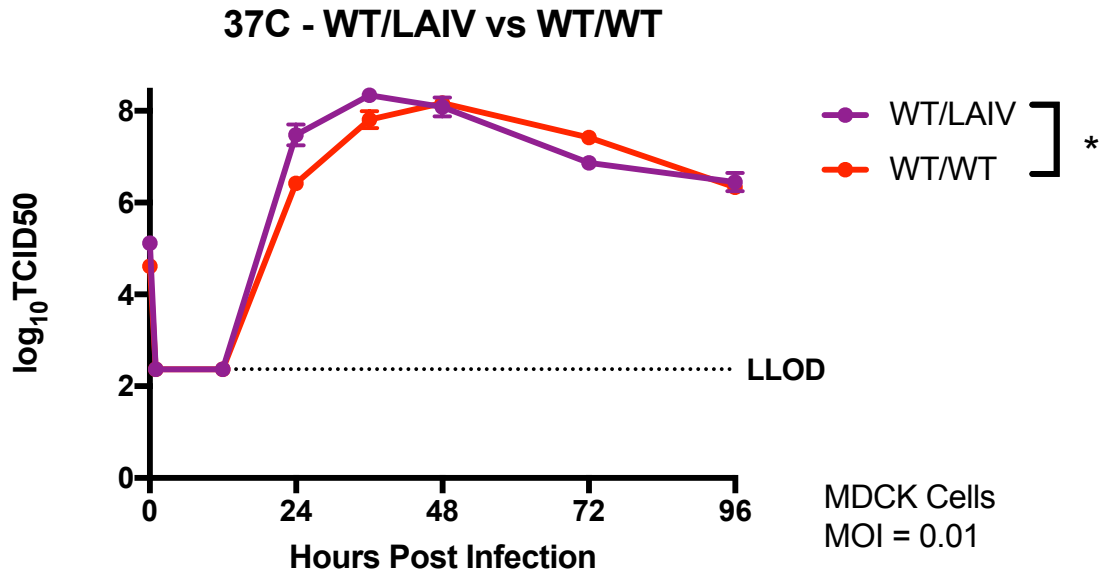
**32C - WT/LAIV vs WT/WT**

Figure 17. Effect of NS Gene Swap in the A/Victoria/361/2011 backbone at 32$^o$C in A549 Cells. A multistep growth curve was performed on MDCK cells with the indicated viruses. Statistical differences were determined by MANOVA followed by Bonferroni post-test. *=P < 0.05; **= P < 0.01; ***=P<0.001. L.O.D=limit of detection=2.37.

### 2.3.5 Replication of NS Reassortant Viruses at 37$^o$C in A549 Cells

Multistep growth curves were also performed at 37$^o$C to evaluate any temperature sensitive phenotypes in the virus panel. The A549 cells were inoculated at an MOI = 0.55.

Similar to what was observed at 32$^o$C, the LAIV/LAIV and LAIV/WT viruses demonstrated no significant differences in replication kinetics at 37$^o$C (Fig. 18). They both reached roughly the same peak titer in the same amount of time. For the WT viruses, however, the WT/LAIV virus reached its peak titer faster than the WT/WT virus. Both viruses achieved roughly the same peak titer (Fig. 19).
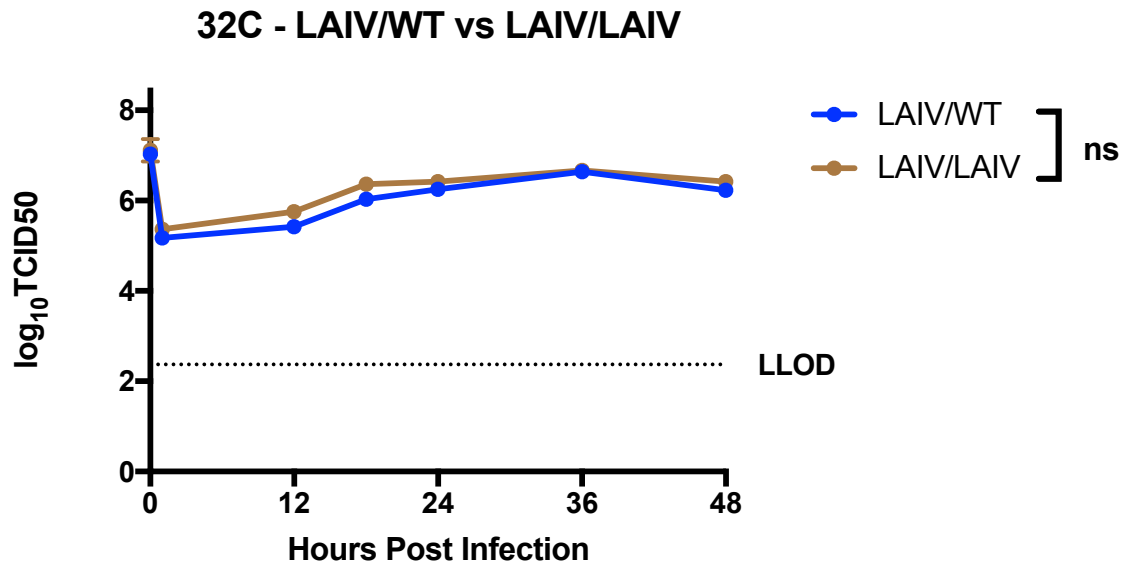
40

**37C - LAIV/WT vs LAIV/LAIV**

Figure 18. Effect of NS Gene Swap in the LAIV backbone at 37$^{o}$C in A549 Cells. A multistep growth curve was performed on MDCK cells with the indicated viruses. Statistical differences were determined by MANOVA followed by Bonferroni post-test. *=P < 0.05; **= P < 0.01; ***=P<0.001. L.O.D=limit of detection=2.37.
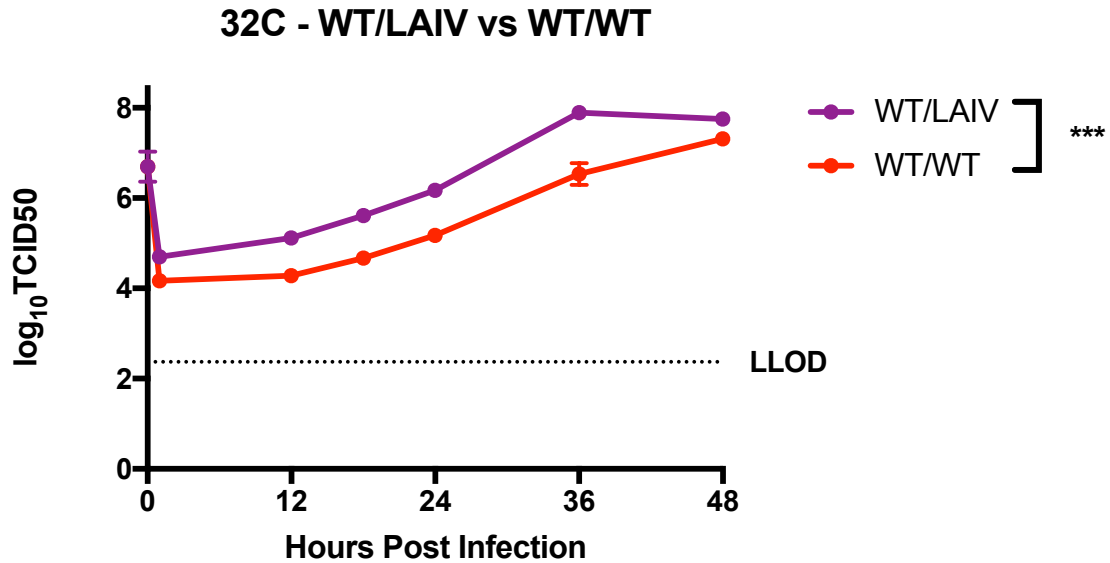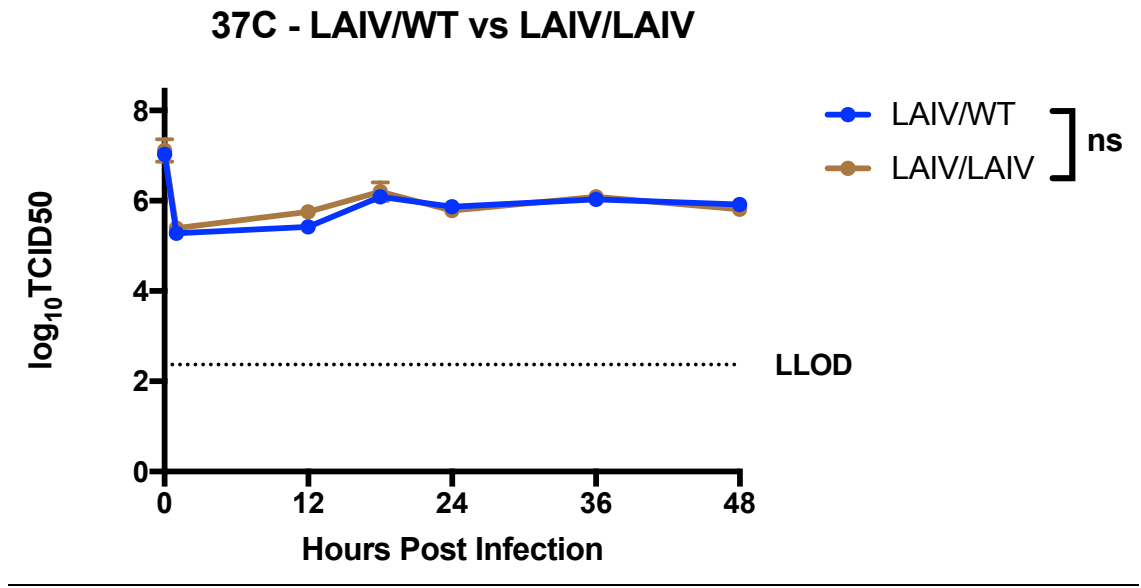
**37C - WT/LAIV vs WT/WT**

Figure 19. Effect of NS Gene Swap in the A/Victoria/361/2011 backbone at $37^{o}$C in A549 Cells. A multistep growth curve was performed on MDCK cells with the indicated viruses. Statistical differences were determined by MANOVA followed by Bonferroni post-test. *=P < 0.05; **= P < 0.01; ***=P<0.001. L.O.D=limit of detection=2.37.

## *2.4 Discussion*

Previous work suggests that mutations which arise in the NS gene during the serial passage process of LAIV may contribute to viral attenuation and/or temperature sensitivity [66]. We examined this through NS gene segment reassortments in a panel of viruses. Although this does not allow us to determine the specific mutations that may contribute to an attenuation phenotype, we would be able to determine what role, if any, the entire gene segment has in viral replication. To test this, we performed several multistep growth curves between the NS reassortant viruses outlined in Table 3.

In MDCK cells at a low MOI (MOI = 0.01), there were significant differences between LAIV/LAIV and LAIV/WT, as well as significant differences between WT/LAIV and WT/WT. In both backbones, the virus with the LAIV NS gene segment had faster

replication kinetics than its wild-type matched NS counterpart. However, all viruses eventually reached roughly the same peak titer. This trend was observed at both 32$^o$C and 37$^o$C, which indicates that the NS gene is not responsible for the temperature sensitive phenotype in cell culture.

We also conducted multistep growth curves at a high MOI (MOI = 0.55) in A549 cells, which represents a more humanized model of infection (compared to canine kidney cells). In the A549 cell culture system, the LAIV-backbone viruses were found to have no significant differences in growth kinetics or peak titer from one another at 32$^o$C or 37$^o$C. In the WT backbone, the WT/LAIV had significantly faster growth at both 32$^o$C and 37$^o$C. At 32$^o$C, the WT/LAIV virus had a higher peak titer (~100 fold greater) than WT/WT. For the WT viruses, these data indicate the NS gene has a role in viral replication. However, in the context of these data, we are unable to determine which of the two proteins encoded by the NS gene, NS1 or NEP, are contributing to this phenotype. NEP is likely to be the larger contributor because it associates with the M2 protein during viral assembly, whereas NS1 primarily antagonizes the innate immune response.


# Chapter 3 - Recombinant influenza expressing mutations at amino acid 153 that are associated with the cold adaptation of live attenuated influenza virus vaccines

## *3.1 Introduction*

### 3.1.1 Interest in aa 153

The genome of LAIV has developed a series of mutations which allow it to survive and propagate at 25$^o$C in embryonated hen's eggs. I wanted to take a deeper look into

how these mutations influence viral growth and replication. Of particular interest is the aa 153 mutation in the NS1 protein. I want to generate a panel of NS1 aa 153 mutant viruses in both the LAIV and circulating wt A/Victoria/361/2011 backbones. This will allow us to determine if the aa 153 mutation first observed by Cox et al. has any influence on the attenuation of LAIV.

### 3.1.2 Virus Mutant Selection

When observing the relative amino acid frequency of current H3N2 human clinical isolates, glutamic acid is by far the most prevalent genotype, accounting for roughly 99% of collected samples.

For our mutations in the A/Victoria/361/2011 backbone, E153 will serve as the baseline genotype. However, when we use the same search parameters for avian species, aspartic acid is the most prevalent phenotype, accounting for roughly three-quarters of isolates. - glutamic acid accounts for the remaining one-quarter of isolates. Although the side chains are very similar in structure and property, it would also be interesting to see what effect a D153 mutation has on virus phenotype.

LAIV exhibits a T153 genotype - this will serve as the baseline amino acid for all work conducted in the LAIV backbone. When compared to the original wt A/Ann Arbor/6/60 clinical isolate, a A153 genotype is observed. I wanted to create mutations in the LAIV backbone that reflect a reversion to the A153 genotype, a conversion to the wt H3N2 E153 genotype, and a conversion to the avian D153 genotype. Furthermore, we will create similar mutations in the A/Victoria/361/2011 backbone that reflect conversions to

the wt A/Ann Arbor/6/60 A153 genotype, LAIV's T153 genotype, and the avian D153 genotype. These viruses are listed in Tables 4 and 5.

| Mutation | Amino Acid | Properties | Structure of Functional Group |
|---|---|---|---|
| E153A | Alanine | Nonpolar, hydrophobic |  |
| E153T | Threonine | Polar, uncharged |  |
| E153D | Aspartic Acid | Acidic |  |

Table 4. Panel of aa 153 Viruses in A/Victoria/361/2011 Backbone

| Mutation | Amino Acid | Properties | Structure of Functional Group |
|---|---|---|---|
| T153A | Alanine | Nonpolar, hydrophobic |  |
| T153E | Glutamic Acid | Acidic |  |
| T153D | Aspartic Acid | Acidic |  |

Table 5. Panel of aa 153 Viruses in LAIV Backbone

| Influenza Strain | Amino Acid | Frequency (%) |
|---|---|---|
| Human H1N1 | Glutamic Acid | 99 |
| Human H3N2 | Glutamic Acid | 99 |
| Avian (all subtypes) | Glutamic Acid | 23 |
| | Aspartic Acid | 76 |

Table 6. Frequency of Amino Acids Isolated from North American Clinical Samples (aa 153)

*3.2 Materials and Methods*

**3.2.1 Cell Lines**

Madin Darby canine kidney (MDCK) cells were maintained in Dulbecco's Modified Eagle's Medium (DMEM) with 10% fetal bovine serum (FBS), 100 U/mL penicillin, 100 ug/mL streptomycin and 2mM L-glutamine at $37^{o}C$ with 5% $CO_2$ and passaged at a 1:10 dilution every 3-4 days.

Transformed human embryonic kidney 293 cells (293T) were maintained in DMEM with 10% fetal bovine serum (FBS), 100 U/mL penicillin, 100 ug/mL streptomycin and 2mM L-glutamine at $37^{o}C$ with 5% $CO_2$ and passaged at a 1:10 dilution every 3-4 days.

**3.2.2 Plasmids**

The pHH21 plasmid for the NS segment encodes the influenza A/Victoria/361/2011 and LAIV NS segment under the control of human RNA polymerase I promoter and murine RNA polymerase I terminator. This pHH21 plasmid encoding the NS segment was mutated using the the Quickchange Site-Directed Mutagenesis Kit (Stratagene) to induce mutations at aa 153. Forward and reverse primers were designed to create desired mutations and their sequences are shown in Table 7 (Integrated DNA Technologies). The pHH21 plasmid and the primers of interest were subjected to PCR. Dpn1 enzyme was used to cleave and remove supercoiled parental plasmid from the PCR mixtures. The purified PCR mixture was transformed into competent bacterial (Ultra Gold) cells. Several bacterial colonies were selected for each mutant and their DNA purified using the QIAprep Spin Miniprep Kit (Qiagen). The DNA was sequenced using the FluA5 and FluA6 primers.

| Plasmid | Forward Primer | Reverse Primer |
|---|---|---|
| pHH21 A/Vic-NS1-E153A | 5' CCA ACA ATT GCT CCG GCT TCG GTG AAA GCC CTT AGT AAT ACT AT 3' | 5' ATA GTA TTA CTA AGG GCT TTC ACC GAA GCC GGA GCA ATT GTT GG 3' |
| pHH21 A/Vic-NS1-E153D | 5' CCA ACA ATT GCT CCG TCT TCG GTG AAA GCC CTT AGT AAT ACT AT 3' | 5' ATA GTA TTA CTA AGG GCT TTC ACC GAA GAC GGA GCA ATT GTT GG 3' |
| pHH21 A/Vic-NS1-E153T | 5' CCA ACA ATT GCT CCC GTT TCG GTG AAA GCC CTT AGT AAT ACT AT 3' | 5' ATA GTA TTA CTA AGG GCT TTC ACC GAA ACG GGA GCA ATT GTT GG 3' |
| pHH21 LAIV-NS1-T153A | 5' CCA ACA ATT GCT CCG GCT TCG GTG AAA GCC CTT AGT AAT AAT AT 3' | 5' CTA ATA TTA CTA AGG GCT TTC ACC GAA GCC GGA GCA ATT GTT GG 3' |
| pHH21 LAIV-NS1-T153D | 5' CCA ACA ATT GCT CCG TCT TCG GTG AAA GCC CTT AGT AAT ATT AT 3' | 5' CTA ATA TTA CTA AGG GCT TTC ACC GAA GAC GGA GCA ATT GTT GG 3' |
| pHH21 LAIV-NS1-T153E | 5' CCA ACA ATT GCT CCC TCT TCG GTG AAA GCC CTT AGT AAT ATT AT 3' | 5' CTA ATA TTA CTA AGG GCT TTC ACC GAA GAG GGA GCA ATT GTT GG 3' |

Table 7. Sequences of Primers used to Generate Recombinant Viruses at aa 153

### 3.2.3 Recombinant Viruses

A 12 plasmid recombinant virus rescue system was utilized to generate the panel viruses (Neumann et al., 1999). 6-well plates were coated with poly-L-lysine and 293T cells were plated at 40-60% confluence 24 hours prior to transfection. For the A/Victoria/361/2011 viruses, 293T cells were transfected with A/Victoria/361/2011 pHH21 plasmids encoding PB2, PB1, PA, NP, NA, HA, M (0.5 µg each) and NS (1.0 µg). For the

48

with the LAIV genome, 293T cells were transfected with LAIV pHH21 plasmids encoding PB2, PB1, PA, NP, NA, HA, M (0.5 µg each) and NS (1.0 µg). All viruses were transfected with helper plasmids under the control of RNA polymerase II promoters encoding A/Udorn/72 PB1, PB2, NP (1µg each) and PA (0.2 µg).

Transfection reagent TransIT-LT-1 (LT1) (Mirus) (20 µL/transfection) was mixed with OptiMEM medium (Gibco) (100 µL/transfection) and incubated at room temperature for 15 minutes. Plasmids were mixed at the aforementioned quantities, added to the LT1/OptiMEM mixture, and incubated at room temperature for another 15 minutes. DMEM was aspirated from 6-well plates containing 293T cells and replaced with 2 mL/well of OptiMEM. The corresponding transfection mix was added dropwise to each well. The plates were incubated at $32^{o}C$ with 5% $CO_2$. 24 hours following transfection, 2.24 µL of 5 µg/mL N-acetyl trypsin (NAT) (Sigma) was added to each well to bring the total concentration of NAT to 10 µg/mL. The cells were incubated at $32^{o}C$ with 5% $CO_2$ for 4 hours and then each well overlaid with approx. $5*10^5$ MDCK cells suspended in 100 µL OptiMEM. The plates were transferred to a $37^{o}C$ incubator. Every 24 hours for approx. five days, 1 mL of supernatant was removed from the cells and replaced with 1 mL DMEM with 4 µg/mL NAT, 100 U/mL penicillin, 100 µg/mL streptomycin, 2mM L-glutamine, and 0.5% bovine serum albumin (BSA) (Sigma) (IM+NAT). Transfection was discontinued when indications of comprehensive cytopathic effects were observed.

### 3.2.4 TCID$_{50}$ Assay

Fifty percent tissue culture infectious dose (TCID$_{50}$) were utilized to determine viral titers. MDCK cells were plated to confluence in 96-well plates. Viral supernatants were diluted at concentrations from $10^{-1}$ to $10^{-8}$ in IM+NAT. 20 µL of each 10-fold dilution was

added to six consecutive wells on a confluent 96-well plate containing MDCK cells. These plates were incubated at $32^{o}C$ with 5% $CO_2$ for 7 days. The cells were fixed with 4% formaldehyde and stained with naphthol blue-black overnight. Cytopathic effects (CPE) were scored visually and $TCID_{50}$ was quantified using the Reed and Muench calculation.

### 3.2.5 Plaque Purification

Recombinant influenza viruses generated following transfection must be purified from the transfection supernatant. 6-well plates were seeded with MDCK cells and seeded to confluence. 100 µL of transfection supernatant was serially diluted ten-fold from $10^{-1}$ to $10^{-8}$ with IM+NAT. 6-well plates were aspirated and washed twice with PBS+. 250 µL of diluted virus (dilutions determined from $TCID_{50}$ of transfection supernatant) was added to each well. The 6-well plates were incubated for one hour at $32^{o}C$ for viruses with LAIV polymerase genes and $37^{o}C$ for viruses with A/Victoria/361/2011 polymerase genes. During the incubation period, the plates were gently tapped every 15 minutes to evenly distribute virus. Following incubation, the inoculum was aspirated and replaced with ∼ 4 mL of a mixture of 2% agarose, 2X Modified Eagle's Medium (MEM), and 4 µg/mL NAT. Plates were incubated at $32^{o}C$ for 72-120 hours. Clear, defined, and singular plaques were picked using a 1 mL serological pipette, placed into tubes containing 500 µL IM, and stored at $-80^{o}C$.

### 3.2.6 Virus Infection to Generate Viral Stocks

MDCK cells were grown to confluence in T150 (150 $cm^2$) flasks. 100 µL of the media from the plaque resuspension was added to 5 mL IM+NAT. The media was

aspirated from the T150 flasks and replaced by the virus and IM mixture. The flasks were incubated for one hour at 32$^o$C for viruses with LAIV polymerase genes and 37$^o$C for viruses with A/Victoria/361/2011 polymerase genes. During the incubation period, the plates were gently tapped every 15 minutes to evenly distribute virus. Following the one hour incubation, the inoculum was aspirated and replaced with 20 mL IM. The cells were monitored daily for CPE and the supernatants harvested after 30-40% of cells were dead or had detached from the flask. 200 µL of supernatant was harvested and used to establish a bank of viral seed stocks. The seed stocks were sequenced to confirm a purified virus product and later titered via TCID$_{50}$ assay. Once viral sequencing was completed, working stocks were generated from the seed stocks (MOI = 0.001) in the manner described above. Working stocks were also titered via TCID$_{50}$ assay.

## *3.3 Results*

### 3.3.1 Rescue of Recombinant Influenza Viruses Encoding NS1 aa 153 Mutations

Viruses encoding a mutation at aa 153 in both the A/Victoria/361/2011 and LAIV backbone were successfully rescued. The NS gene was sequenced to confirm presence of desired aa 153 mutation. The seven remaining gene segments were sequenced to ensure there were no incidental mutations that occurred during the transfection process.

## *3.4 Discussion*

Unfortunately, due to time constraints, the viral growth kinetics of the aa 153 viruses could not be evaluated. However, a panel of these viruses in both the LAIV and

A/Victoria/361/2011 backbones were generated, sequenced, and aliquoted into seed stocks for a future thesis project.


# Chapter 4 – Conclusion and Future Directions

Previous research conducted in our lab demonstrated that in human nasal epithelial cells at 32$^{\circ}$C, wild-type A/Victoria/361/2011 reached higher peak titers at a faster rate than LAIV. For my NS reassortant viruses, I would have anticipated this trend to remain the same, and those reassortants with the wild-type NS to have faster growth kinetics than the lineage-matched reassortant with LAIV NS. However, the opposite trend was observed and those reassortants with LAIV NS had faster growth kinetics than the reassortants with wild-type NS. These data indicate the NS gene may play a role in influenza replication.

Since LAIV is developed in embryonated hen's eggs, we believe we can apply this project to an avian model. We could study NS gene reassortment in embryonated hen's eggs or primary chick fibroblasts and compare that to our data in A549 cells. Ideally, we would like to conduct research in a more humanized model like human nasal epithelial cells and/or human tracheal cells and compare that to avian cells. Based off the data presented in this project, I'd expect the reassortant viruses with LAIV NS to have faster growth kinetics than the viruses with wild-type NS in a human model. I would expect the same in an avian model. LAIV has adapted to replicate efficiently within embryonated hen's eggs whereas wild-type viruses have adapted to growth within epithelial cells. In an avian model, viruses with LAIV NS would likely have a replication advantage.

The data presented in this project primarily investigated the role of the NS gene in viral replication, however we know one of its encoded proteins, NS1, is an immune system antagonist. We believe the NS reassortment viruses should also be evaluated for their innate immune inhibition. Reporter gene assays will allow us to measure the induction of cellular signaling pathways including NF-KB, JAK/STAT, and MAPK. We can also take a more in depth look at innate immune responses by specifically measuring known viral response factors including IRF3/7 phosphorylation and Type I and III interferon induction. Furthermore, we'd like to analyze the chemokines and cytokines that are secreted in human nasal epithelial cells in response to influenza infection. When taken from harvested supernatants from a growth curve, we can look at what/when chemokines and cytokines are excreted after being infected with influenza. Furthermore, since these cells are polarized, we can compare the apical and basolateral media to see if there are any differences in secretion. Analyzing the supernatants for specific chemokines and cytokines will provide insight into what innate immune cells may be recruited to combat influenza infection.

Although time constraints prevented characterization of the aa 153 recombinant viruses, we can still hypothesize how they might replicate in humanized cells. For the wild-type viruses, I'd expect E153A to have the fastest growth kinetics, as this is the amino acid found at residue 153 in the A/Ann Arbor/6/60 wild-type virus. The other mutation, E153T, represents the LAIV sequence. Since other point mutations within the LAIV genome have been connected to attenuation and temperature-sensitive phenotypes, we believe the same would be true for our viruses, and predict that E153T would likely confer a degree of attenuation. For the LAIV viruses, there is less experimental evidence to

predict how these mutations would affect their growth. 153A is the WT A/Ann Arbor/6/60 sequences and 153E is found in currently circulating H3N2 viruses.

We believe this work can be applied to the development of an adapted LAIV vaccine strain. Based on the data in this project, it's important to keep the LAIV polymerase genes as the core of the virus – this confers a temperature sensitive phenotype that inhibits the virus from replicating at 37$^{o}$C. However, our data indicates that a wild-type NS gene should be swapped with the LAIV NS. Our LAIV NS reassortant viruses had faster growth rates and even significantly higher titers than the viruses with wild-type NS. For a LAIV vaccine strain, we want a virus that is both temperature sensitive and attenuated – a virus with LAIV polymerase genes and a wild-type NS fits both of these criteria.

# Bibliography

1.      Potter CW. A history of influenza. *J Appl Microbiol*. 2001;91(4):572-579.

2.      Patterson KD, Pyle GF. The diffusion of influenza in sub-Saharan Africa during the 1918–1919 pandemic. *Social Science & Medicine*. 1983;17(17):1299-1307. doi:10.1016/0277-9536(83)90022-9.

3.      Taubenberger JK, Morens DM. 1918 Influenza: the mother of all pandemics. *Emerging Infect Dis*. 2006;12(1):15-22. doi:10.3201/eid1201.050979.

4.      Simonsen L, Clarke MJ, Schonberger LB, Arden NH, Cox NJ, Fukuda K. Pandemic versus epidemic influenza mortality: a pattern of changing age distribution. *J Infect Dis*. 1998;178(1):53-60.

5.      Bouvier NM, Palese P. The biology of influenza viruses. *Vaccine*. 2008;26 Suppl 4(Suppl 4):D49-D53.

6.      Xie Z, Pang Y-S, Liu J, et al. A multiplex RT-PCR for detection of type A influenza virus and differentiation of avian H5, H7, and H9 hemagglutinin subtypes. *Mol Cell Probes*. 2006;20(3-4):245-249. doi:10.1016/j.mcp.2006.01.003.

7.      Molinari N-AM, Ortega-Sanchez IR, Messonnier ML, et al. The annual impact of seasonal influenza in the US: measuring disease burden and costs. *Vaccine*. 2007;25(27):5086-5096. doi:10.1016/j.vaccine.2007.03.046.

8.      Wong KK, Jain S, Blanton L, et al. Influenza-associated pediatric deaths in the United States, 2004-2012. *Pediatrics*. 2013;132(5):796-804. doi:10.1542/peds.2013-1493.

9.      Kostova D, Reed C, Finelli L, et al. Influenza Illness and Hospitalizations Averted by Influenza Vaccination in the United States, 2005-2011. Goldstein E, ed. *PLoS ONE*. 2013;8(6):e66312. doi:10.1371/journal.pone.0066312.

10.     Mertz D, Kim TH, Johnstone J, et al. Populations at risk for severe or complicated influenza illness: systematic review and meta-analysis. *BMJ*. 2013;347(aug23 1):f5061-f5061. doi:10.1136/bmj.f5061.

11.     Thompson WW, Shay DK, Weintraub E, et al. Influenza-associated hospitalizations in the United States. *JAMA*. 2004;292(11):1333-1340. doi:10.1001/jama.292.11.1333.

12.     Dushoff J, Plotkin JB, Viboud C, Earn DJD, Simonsen L. Mortality due to influenza in the United States--an annualized regression approach using multiple-cause mortality data. *Am J Epidemiol*. 2006;163(2):181-187. doi:10.1093/aje/kwj024.

13.     Mosby LG, Rasmussen SA, Jamieson DJ. 2009 pandemic influenza A (H1N1) in pregnancy: a systematic review of the literature. *Am J Obstet Gynecol*.

2011;205(1):10-18. doi:10.1016/j.ajog.2010.12.033.

14. Robinson DP, Klein SL. Pregnancy and pregnancy-associated hormones alter immune responses and disease pathogenesis. *Horm Behav*. 2012;62(3):263-271. doi:10.1016/j.yhbeh.2012.02.023.

15. Kunisaki KM, Janoff EN. Influenza in immunosuppressed populations: a review of infection frequency, morbidity, mortality, and vaccine responses. *Lancet Infect Dis*. 2009;9(8):493-504. doi:10.1016/S1473-3099(09)70175-6.

16. Nair H, Brooks WA, Katz M, et al. Global burden of respiratory infections due to seasonal influenza in young children: a systematic review and meta-analysis. *Lancet*. 2011;378(9807):1917-1930. doi:10.1016/S0140-6736(11)61051-9.

17. Couceiro JN, Paulson JC, Baum LG. Influenza virus strains selectively recognize sialyloligosaccharides on human respiratory epithelium; the role of the host cell in selection of hemagglutinin receptor specificity. *Virus Res*. 1993;29(2):155-165.

18. Matrosovich MN, Matrosovich TY, Gray T, Roberts NA, Klenk H-D. Human and avian influenza viruses target different cell types in cultures of human airway epithelium. *Proc Natl Acad Sci USA*. 2004;101(13):4620-4624. doi:10.1073/pnas.0308001101.

19. Sieczkarski SB, Whittaker GR. Viral entry. *Curr Top Microbiol Immunol*. 2005;285:1-23.

20. Cros JF, Palese P. Trafficking of viral genomic RNA into and out of the nucleus: influenza, Thogoto and Borna disease viruses. *Virus Res*. 2003;95(1-2):3-12.

21. Krug RM. Priming of influenza viral RNA transcription by capped heterologous RNAs. *Curr Top Microbiol Immunol*. 1981;93:125-149.

22. Li X, Palese P. Characterization of the polyadenylation signal of influenza virus RNA. *J Virol*. 1994;68(2):1245-1249.

23. Colman PM, Varghese JN, Laver WG. Structure of the catalytic and antigenic sites in influenza virus neuraminidase. *Nature*. 1983;303(5912):41-44.

24. revisionofthesystemofnomenclaturefor influenzaviruses:. February 2008:1-7.

25. Cox NJ, Subbarao K. Influenza. *Lancet*. 1999;354(9186):1277-1282. doi:10.1016/S0140-6736(99)01241-6.

26. Thompson WW, Weintraub E, Dhankhar P, et al. Estimates of US influenza-associated deaths made using four different methods. *Influenza Other Respir Viruses*. 2009;3(1):37-49. doi:10.1111/j.1750-2659.2009.00073.x.

27. Dowell SF. Seasonal variation in host susceptibility and cycles of certain infectious diseases. *Emerging Infect Dis*. 2001;7(3):369-374. doi:10.3201/eid0703.010301.

28. Hayes CE, Nashold FE, Spach KM, Pedersen LB. The immunological functions of the vitamin D endocrine system. *Cell Mol Biol (Noisy-le-grand)*. 2003;49(2):277-300.

29. Burström B, Diderichsen F, Smedman L. Child mortality in Stockholm during 1885-1910: the impact of household size and number of children in the family on the risk of death from measles. *Am J Epidemiol*. 1999;149(12):1134-1141.

30. Foxman EF, Storer JA, Fitzgerald ME, et al. Temperature-dependent innate defense against the common cold virus limits viral replication at warm temperature in mouse airway cells. *Proc Natl Acad Sci USA*. 2015;112(3):827-832. doi:10.1073/pnas.1411030112.

31. Lowen AC, Steel J. Roles of humidity and temperature in shaping influenza seasonality. Schultz-Cherry S, ed. *J Virol*. 2014;88(14):7692-7695. doi:10.1128/JVI.03544-13.

32. Gerdil C. The annual production cycle for influenza vaccine. *Vaccine*. 2003;21(16):1776-1779.

33. Kilbourne ED, Schulman JL, Schild GC, Schloer G, Swanson J, Bucher D. Related studies of a recombinant influenza-virus vaccine. I. Derivation and characterization of virus and vaccine. *J Infect Dis*. 1971;124(5):449-462.

34. NCIRD C. Vaccine Information Statement: Inactivated Influenza Vaccine. August 2015:1-2.

35. Neuzil KM, Dupont WD, Wright PF, Edwards KM. Efficacy of inactivated and cold-adapted vaccines against influenza A infection, 1985 to 1990: the pediatric experience. *Pediatr Infect Dis J*. 2001;20(8):733-740.

36. NCIRD C. Vaccine Information Statement: Attenuated Influenza Vaccine, Live, Intranasal. August 2015:1-2.

37. Boyce TG, Gruber WC, Coleman-Dockery SD, et al. Mucosal immune response to trivalent live attenuated intranasal influenza vaccine in children. *Vaccine*. 1999;18(1-2):82-88.

38. Wong S-S, Webby RJ. Traditional and new influenza vaccines. *Clin Microbiol Rev*. 2013;26(3):476-492. doi:10.1128/CMR.00097-12.

39. Schodel M. STN 125408-101 PI Approved Final Draft. May 2016:1-19.

40. Nolan T, Chotpitayasunondh T, Capeding MR, et al. Safety and tolerability of a cell culture derived trivalent subunit inactivated influenza vaccine administered to healthy children and adolescents: A Phase III, randomized, multicenter, observer-blind study. *Vaccine*. 2016;34(2):230-236. doi:10.1016/j.vaccine.2015.11.040.

41. Jarvis DL. Baculovirus-insect cell expression systems. *Meth Enzymol*. 2009;463:191-222. doi:10.1016/S0076-6879(09)63014-7.

42.    McPherson CE. Development of a novel recombinant influenza vaccine in insect cells. *Biologicals*. 2008;36(6):350-353. doi:10.1016/j.biologicals.2008.08.001.

43.    Lin D, Lan J, Zhang Z. Structure and function of the NS1 protein of influenza A virus. *Acta Biochim Biophys Sin (Shanghai)*. 2007;39(3):155-162.

44.    Wang W, Riedel K, Lynch P, Chien CY, Montelione GT, Krug RM. RNA binding by the novel helical domain of the influenza virus NS1 protein requires its dimer structure and a small number of specific basic amino acids. *RNA*. 1999;5(2):195-205.

45.    Silverman RH. Viral encounters with 2",5-"oligoadenylate synthetase and RNase L during the interferon antiviral response. *J Virol*. 2007;81(23):12720-12729. doi:10.1128/JVI.01471-07.

46.    Min J-Y, Krug RM. The primary function of RNA binding by the influenza A virus NS1 protein in infected cells: Inhibiting the 2"-5" oligo (A) synthetase/RNase L pathway. *Proc Natl Acad Sci USA*. 2006;103(18):7100-7105. doi:10.1073/pnas.0602184103.

47.    Stasakova J, Ferko B, Kittel C, et al. Influenza A mutant viruses with altered NS1 protein function provoke caspase-1 activation in primary human macrophages, resulting in fast apoptosis and release of high levels of interleukins 1beta and 18. *J Gen Virol*. 2005;86(Pt 1):185-195. doi:10.1099/vir.0.80422-0.

48.    Carrillo B, Choi J-M, Bornholdt ZA, Sankaran B, Rice AP, Prasad BVV. The influenza A virus protein NS1 displays structural polymorphism. *J Virol*. 2014;88(8):4113-4122. doi:10.1128/JVI.03692-13.

49.    Long J-X, Peng D-X, Liu Y-L, Wu Y-T, Liu X-F. Virulence of H5N1 avian influenza virus enhanced by a 15-nucleotide deletion in the viral nonstructural gene. *Virus Genes*. 2008;36(3):471-478. doi:10.1007/s11262-007-0187-8.

50.    Bornholdt ZA, Prasad BVV. X-ray structure of influenza virus NS1 effector domain. *Nat Struct Mol Biol*. 2006;13(6):559-560. doi:10.1038/nsmb1099.

51.    Hale BG, Randall RE, Ortín J, Jackson D. The multifunctional NS1 protein of influenza A viruses. *J Gen Virol*. 2008;89(Pt 10):2359-2376. doi:10.1099/vir.0.2008/004606-0.

52.    Nemeroff ME, Barabino SM, Li Y, Keller W, Krug RM. Influenza virus NS1 protein interacts with the cellular 30 kDa subunit of CPSF and inhibits 3'end formation of cellular pre-mRNAs. *Mol Cell*. 1998;1(7):991-1000.

53.    Reich S, Guilligay D, Pflug A, et al. Structural insight into cap-snatching and RNA synthesis by influenza polymerase. *Nature*. 2014;516(7531):361-366. doi:10.1038/nature14009.

54.    Twu KY, Noah DL, Rao P, Kuo R-L, Krug RM. The CPSF30 binding site on the NS1A protein of influenza A virus is a potential antiviral target. *J Virol*.

2006;80(8):3957-3965. doi:10.1128/JVI.80.8.3957-3965.2006.

55.    Das K, Ma L-C, Xiao R, et al. Structural basis for suppression of a host antiviral response by influenza A virus. *Proc Natl Acad Sci USA*. 2008;105(35):13093-13098. doi:10.1073/pnas.0805213105.

56.    Ayllon J, García-Sastre A. The NS1 protein: a multitasking virulence factor. *Curr Top Microbiol Immunol*. 2015;386(Chapter 400):73-107. doi:10.1007/82_2014_400.

57.    Li Y, Chen ZY, Wang W, Baker CC, Krug RM. The 3'-end-processing factor CPSF is required for the splicing of single-intron pre-mRNAs in vivo. *RNA*. 2001;7(6):920-931.

58.    García MA, Gil J, Ventoso I, et al. Impact of protein kinase PKR in cell biology: from antiviral to antiproliferative action. *Microbiol Mol Biol Rev*. 2006;70(4):1032-1060. doi:10.1128/MMBR.00027-06.

59.    Goodman AG, Smith JA, Balachandran S, et al. The cellular protein P58IPK regulates influenza virus mRNA translation and replication through a PKR-mediated mechanism. *J Virol*. 2007;81(5):2221-2230. doi:10.1128/JVI.02151-06.

60.    Min J-Y, Li S, Sen GC, Krug RM. A site on the influenza A virus NS1 protein mediates both inhibition of PKR activation and temporal regulation of viral RNA synthesis. *Virology*. 2007;363(1):236-243. doi:10.1016/j.virol.2007.01.038.

61.    Li S, Min J-Y, Krug RM, Sen GC. Binding of the influenza A virus NS1 protein to PKR mediates the inhibition of its activation by either PACT or double-stranded RNA. *Virology*. 2006;349(1):13-21. doi:10.1016/j.virol.2006.01.005.

62.    DeBorde DC, Donabedian AM, Herlocher ML, Naeve CW, Maassab HF. Sequence comparison of wild-type and cold-adapted B/Ann Arbor/1/66 influenza virus genes. *Virology*. 1988;163(2):429-443.

63.    Smith H, Sweet C. Lessons for human influenza from pathogenicity studies with ferrets. *Rev Infect Dis*. 1988;10(1):56-75.

64.    Maassab HF, Kendal AP, Abrams GD, Monto AS. Evaluation of a cold-recombinant influenza virus vaccine in ferrets. *J Infect Dis*. 1982;146(6):780-790.

65.    He W, Wang W, Han H, Wang L, Zhang G, Gao B. Molecular basis of live-attenuated influenza virus. Ho PL, ed. *PLoS ONE*. 2013;8(3):e60413. doi:10.1371/journal.pone.0060413.

66.    Cox NJ, Kitame F, Kendal AP, Maassab HF, Naeve C. Identification of sequence changes in the cold-adapted, live attenuated influenza vaccine strain, A/Ann Arbor/6/60 (H2N2). *Virology*. 1988;167(2):554-567.

67.     Forero_etal_2016 final. May 2016:1-29.

68.    DeDiego ML, Nogales A, Lambert-Emo K, Martinez-Sobrido L, Topham DJ. NS1
       Protein Mutation I64T Affects Interferon Responses and Virulence of Circulating
       H3N2 Human Influenza A Viruses. Schultz-Cherry S, ed. *J Virol*.
       2016;90(21):9693-9711. doi:10.1128/JVI.01039-16.

69.    de Silva UC, Tanaka H, Nakamura S, Goto N, Yasunaga T. A comprehensive
       analysis of reassortment in influenza A virus. *Biol Open*. 2012;1(4):385-390.
       doi:10.1242/bio.2012281.

# Curriculum Vitale

# James E. Stanton

**307 Sheep Pasture Rd., Waynesville, NC 28785 ● (828) 400-9468 ●
jstanton828@gmail.com**

---

## EDUCATION

**Johns Hopkins Bloomberg School of Public Health, Baltimore, MD**
- *Master of Science (ScM)*, May 2017; GPA 3.75/4.0
- *Concentration:* Molecular Microbiology and Immunology
- *Research Focus:* Studied the Live Attenuated Influenza Vaccine virus and the influence of its NS1 protein on viral replication and inhibition of host innate immune responses

**University of North Carolina Asheville, Asheville, NC**
- *Bachelor of Science in Chemistry*, May 2014; GPA 3.23/4.0
- *Concentration:* Biochemistry
- *Honors*: University Scholar, University Research Scholar, Deans List Spring 2012, Laurels Scholar

## EMPLOYMENT HISTORY

**Occupational Health Technician**        Feb. 2014 - Aug. 2015
Pardee Urgent Care, Hendersonville, NC
- Triaged and communicated patient's chief complaint/medical history to providers
- Executed basic laboratory procedures including strep throat and flu tests, casting of strained/broken limbs, administration of EKGs, cleaning and dressing of wounds, etc.
- Administered urine drug screens and breath alcohol tests to business and industry clients
- Obtained certification in Basic Life Support.

**Undergraduate Research Associate**        May 2012 - May 2014
UNC Asheville, Asheville, NC
- Undertook original, student-driven research that focused on synthesizing phenstatin analogues - a group of molecules believed to inhibit cancer cell division.
- Techniques utilized included: reflux, aldol condensation, Hemetsberger-Knittel thermolysis, silica gel column chromatography, various workup and separatory techniques for compound purification, and analysis via infrared, proton NMR, and carbon NMR spectroscopy
- Research published in the 2014 UNC Asheville Journal of Undergraduate Research

**Student Events Coordinator**        October 2011- May 2013
UNC Asheville Alumni Relations, Asheville, NC
- Assisted in preparation and set-up of events for Alumni Relations including gathering materials and preparing handouts/informational materials for the event
- Networked with area alumni to re-establish connections with the university and to aid in raising

donations

**Co-owner, Farmer**                                                                                   May 2010- May 2014
Stray Cat Farms, Waynesville, NC
- Managed a small family farm with my father that focused on growing organic produce
- Grew and tended to crops including tomatoes, onions, beans, potatoes, squash, zucchini, and a variety of other vegetables
- Sold the produce at a local farmer's market and managed the farm's finances

## COMMUNITY SERVICE EXPERIENCE

**Adolescent Sexual Education Teacher**                                               Sept. 2015- Dec. 2015
Baltimore City Public Schools, Baltimore, MD
- Worked as an educator through Community Adolescent Sexual Education (CASE) to provide a comprehensive sexual education course for 8th grade boys in the Baltimore City Public Schools
- Taught a variety of aspects including: basic anatomy, contraception, sexually transmitted infections, sexual orientation, healthy body image, and sexual consent

**Peer Tutor**                                                                                        Jan. 2014 - Aug. 2015
Urban Mentoring Academy, Asheville, NC
- Serve as a peer tutor to elementary and middle school students who reside in an underserved, public housing neighborhood in the city of Asheville.
- Tutor in a variety of subjects including reading comprehension, math, science, etc.
- Helped in enrichment activities prior to the start of the program where the students would learn about the structure of the local government, famous figures in African American History, and the importance of certain current events

## LEADERSHIP EXPERIENCE

**Board Member**                                                                                   May 2013- May 2014
Senior Class Board, UNC Asheville
- Enhanced the final year of college for seniors at UNC Asheville by hosting events to bolster school spirit
- Organized the Senior Class Campaign through which Board Members were tasked with raising donations from graduating seniors. Students could elect to have their money go to a specific department or athletic team, or to the scholarship fund for the university

**Member**                                                                                           May 2013- May 2014
Order of Pisgah, UNC Asheville
- Served as a personal ambassador for the Chancellor at university events she hosts at her residence
- Communicated my experience at UNC Asheville in order to engage and network with donors of the university

**Vice President of Finance**                                                                    June 2011- May 2013
Student Alumni Association, UNC Asheville
- Founding Board Member
- Organized the Nearly Naked Mile - the official kick-off event for Homecoming through which students donate their gently used clothing to a local homeless shelter and participate in a one-mile

fun run around campus in nothing but their underwear
- Over the past four years, the event has averaged 200 participants and over 1000 articles of donated clothing per year. Awarded Innovative Student Program of the Year in 2012.

**Orientation Leader**                                                      January 2011- August 2013

Embark Orientation Blue Crew, UNC Asheville
- Met and introduced the incoming freshman class to UNC Asheville
- Lead and organized a variety of events and activities designed to promote socialization between the freshmen
- Helped freshmen register for classes, gave lectures about university resources, and became a contact for questions between the end of orientation in June and the beginning of classes in August.

**President, Vice-President, Treasurer**                              September 2010- May 2014

Sigma Nu Fraternity, Asheville, NC
- Managed chapter internal operations while working with university staff to continue to maintain and improve the chapter's finances, risk reduction policy, member morale, and social involvement.
- Brother of the Year in 2012 and 2014

Figure 1. Positive Influenza Infection Tests in the Northern Hemisphere during 2016-2017. WHO, 2017
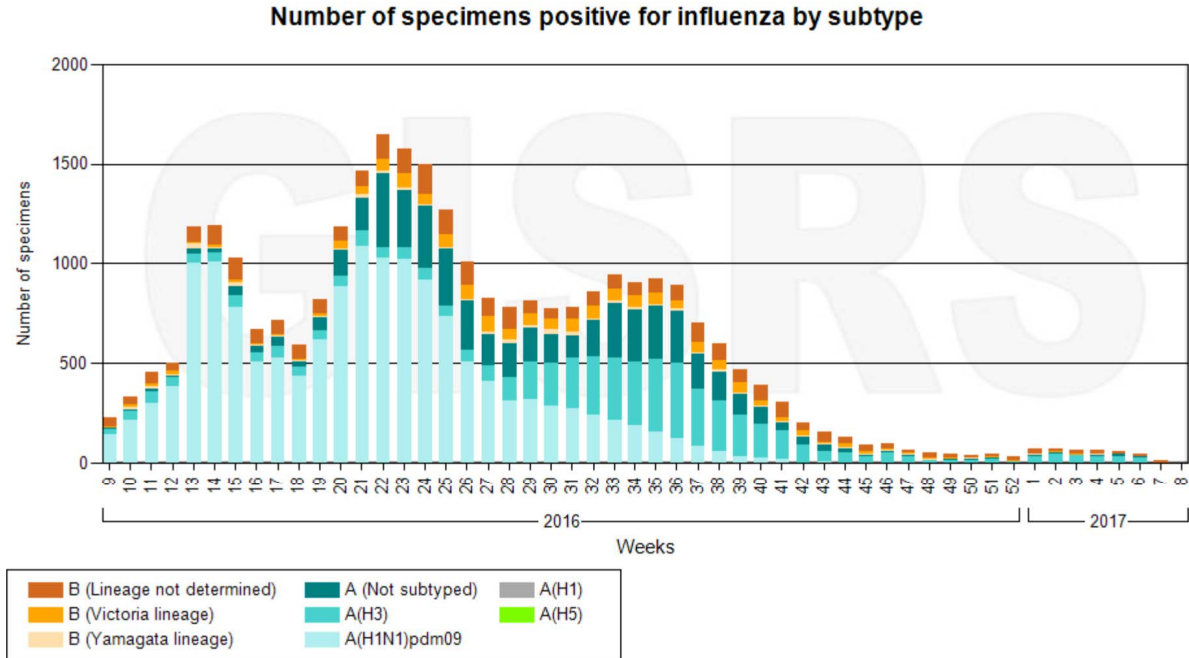
Figure 2. Positive Influenza Infection Tests in the Southern Hemisphere during 2016-2017. WHO, 2017

Unfortunately for epidemiologists and public health professionals, there is no discrete, singular reason why influenza infections peak during the winter months. One theory posits that serum levels of Vitamin D drop during this time as people are less likely to be outside[27]. Vitamin D has been connected to promoting mucosal and CD4+ T cell responses, so influenza may be able to infect hosts more readily as Vitamin D levels drop [28]. Some believe the seasonality of flu is related to social and behavioral factors including crowding which helps transmission by exposing more people to the aerosolized droplets of an infected individual [29]. A new theory suggests that the innate immune response is dampened by a drop in ambient temperature. Foxman et al. demonstrated that rhinovirus is able to infect humans more readily at 33° C due to diminished response by Type I interferons [30]. It would be particularly interesting to see if lowered ambient temperatures

In European countries, finalized vaccine candidates must undergo clinical studies to prove their safety and immunogenicity - this is not required in the United States.
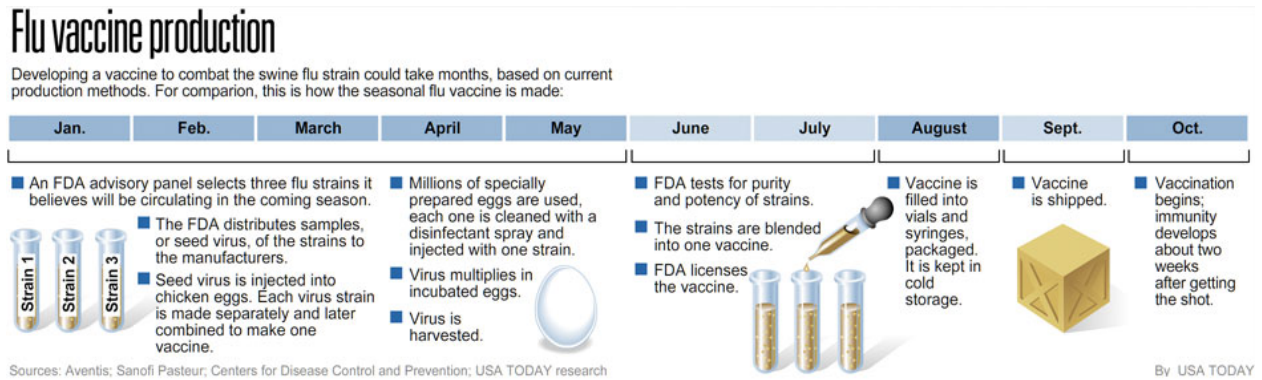


Figure 3. Flu Vaccine Development Timeline for the Northern Hemisphere. USA Today, 2009

### 1.3.2 Vaccine Composition

There are two formulations for the annual vaccine. The most common is the injectable formulation that contains formalin-inactivated virions[34]. These virions have no ability to replicate within the host, but are capable of inducing a memory response by the immune system. The inactivated vaccine has greatest efficacy in patients above the age of 6 [35]. The increased efficacy in older children is most likely attributable to past infection with influenza virus.

The other formulation is a live attenuated influenza vaccine (LAIV) that is administered through a nasal spray into the nasopharyngeal region of the upper respiratory tract[36]. As the name implies, this is a live virus that can replicate within the host, but does not cause disease. This area of the body maintains a temperature around $32^oC$ which permits localized viral growth, but prevents systemic infection into the lower airways which maintain a temperature around $37^oC$. LAIV is of note because its administration has been connected to a broad and systemic IgA mucosal response to not

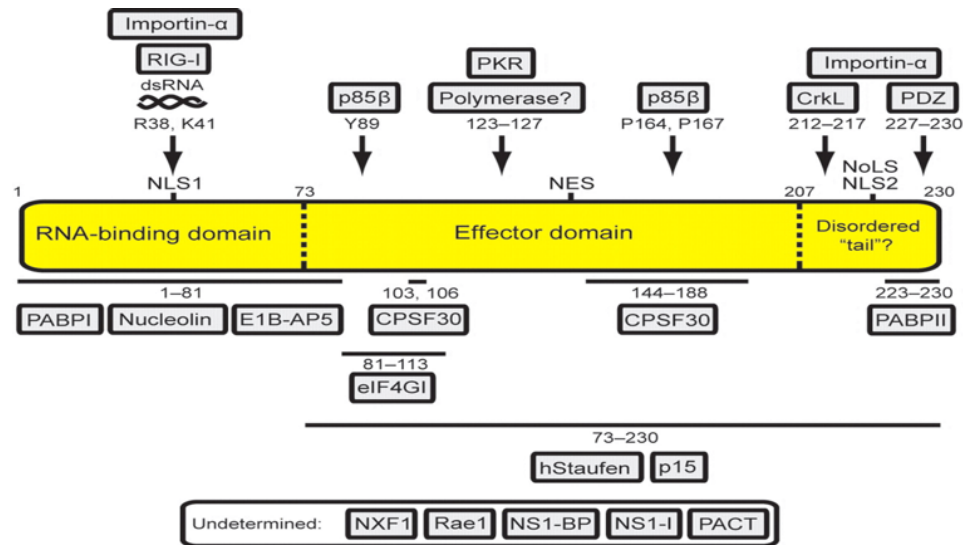also known as the RNA-binding domain, and then the C-terminal domain, also known as the effector domain [43].



Figure. 4. Structure of the NS1 Protein and Cellular Targets of Immune Inhibition. Hale et al., 2005

### 1.4.2 Structure and Function of the N-terminal Domain

The N-terminal domain is roughly defined as amino acids 1-73 of the NS1 protein. As mentioned previously, the N-terminal domain of NS1 is responsible for directly binding host RNA and preventing its transcription into proteins. The N-terminal domain forms a homodimer in solution that consists of three α-helical domains which constitute the majority of secondary structure for this region of the protein. This dimerization is crucial for RNA binding. The α-helices of the homodimer form a unique chain fold that binds RNA between the 2 and 2' chains [43]. Research has determined that within the second α-helix, R38 and K41 are the two crucial amino acids needed for RNA-binding [44]

The NS1 N-terminal domain is well-known for inhibiting the 2'-5' oligoadenylate synthetase (OAS)/RNAse L pathway. The OAS/RNAse L pathway is activated by IL-1β, a
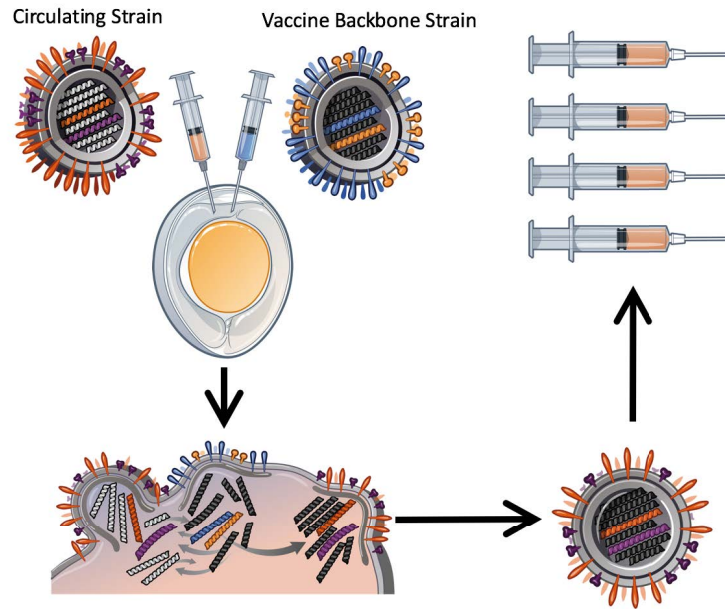
Figure 5. Formulation of LAIV. Modified from NIAID.

### 1.5.3 NS1 Mutations in LAIV

It's clear that point mutations are responsible for the attenuation and temperature restriction of LAIV. Most of the mutations occur in the genes encoding viral polymerases, however a few have been discovered elsewhere in the genome, notably in the NS gene.

Work conducted by Cox et al. mapped one mutation in the coding region of the NS gene segment. Occurring at amino acid 153, the mutation from an alanine (wt) to a threonine (LAIV) was the only difference in the coding region of the NS gene of cold adapted A/Ann Arbor/6/60 when compared to the wt [66]. When examined in the same context as some of the other gene segments, it's reasonable to infer that the mutation at aa 153 of NS might have a role in LAIV attenuation.

| Segment | Coding Changes | Mutation | Effect |
|---|---|---|---|
| PB2 | 1 | N265S | Attenuation, Temp. Sensitivity |
| PB1 | 4 | K391E, E457D, E581G, A661T | Attenuation, Temp. Sensitivity |
| PA | 2 | K613E, L715P | Cold Adaptation, Attenuation |
| NP | 2 | T23N, A34G | ? |
| M | 1 | A86S | Attenuation |
| NS | 1 | A153T | ? |

Table 2. Mutations in A/Ann Arbor/6/60 Arising During the Serial Passage and Cold Adaptation Process

## 1.5.4 Previous Data

Work conducted by Fenstermacher and Forero examined the growth kinetics of HA/NA-antigenically matched LAIV and wt A/Victoria/361/2011 in cultures of human nasal epithelial cells (hNECs) at 33$^{\circ}$C. They found that over a seven day period, infectious particle production as well as growth rate in LAIV was less than its wt counterpart [67].

In addition to altered growth kinetics, LAIV differentially induces the host innate immune response when compared to a wt virus. When hNEC cells were infected at a high multiplicity of infection (MOI), LAIV induced a larger number of genes distinct from the wt virus.
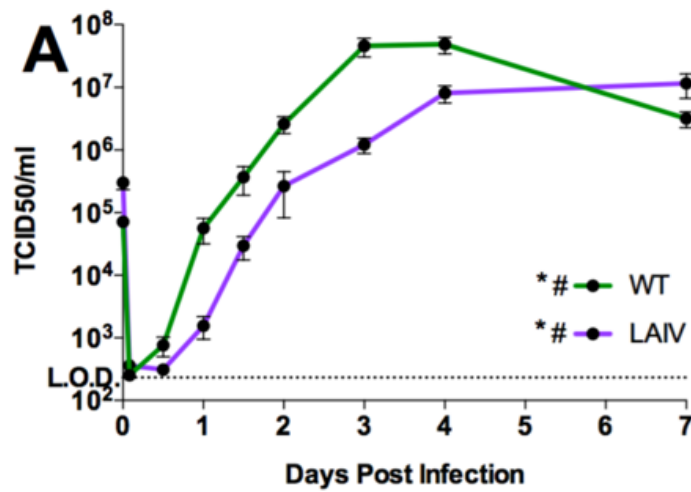
Figure 6. LAIV Demonstrates Altered Growth Kinetics when Compared to wt A/Victoria/361/2011. Forero and Fenstermacher et al., ahead of print.
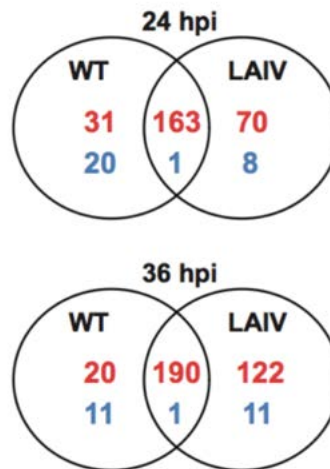


Figure 7. LAIV Differentially Induces the Immune Response. Forero and Fenstermacher et al., ahead of print.

At 24 hours post infection, LAIV induces over twice the amount of unique genes when compared to the wt. Furthermore, at 36 hours post infection, LAIV induces six times

of both its parental viruses which can have a profound impact on virulence within a naive host.

This process of reassortment is commonly known as genetic shift when it involves the HA gene segment and is a hallmark of influenza diversity and adaptation. Many pandemic strains have formed as a result of gene reassortment including the 1918 H1N1, 1957 H2N2, 1968 H3N2, and most recently 2009 H1N1 outbreak. A closer look at the 1918 pandemic strain shows the acquisition of an avian HA gene which drastically enhanced virulence when compared to its original lineage (Pappas et al. 2007).



Figure 8. Hypothetical Reassortment of Influenza within a Swine Host. Stevens et al., 2006.

## 2.1.2 Reassortant Viruses in the Laboratory

In the laboratory, we are able to manually induce gene reassortment to create new influenza viruses. In fact, this is done on an annual basis with LAIV which contains the six internal cold adapted genes from the attenuated virus, as well as the two external genes

27

from the circulating virus subtypes. When a single segment is substituted for another, the resulting virus is referred to as a "7:1 virus" to represent the seven original segments and the one transplant segment. These reassortant viruses are useful in determining the influence of a particular segment on viral phenotype. For example, the aforementioned work conducted by Pappas et al. was done with reassorted H1N1 viruses to elucidate that HA was the crucial segment conferring enhanced virulence in the 1918 pandemic strain. For the purposes of this project, we intend to do NS gene swaps between LAIV and wt A/Victoria/361/2011.

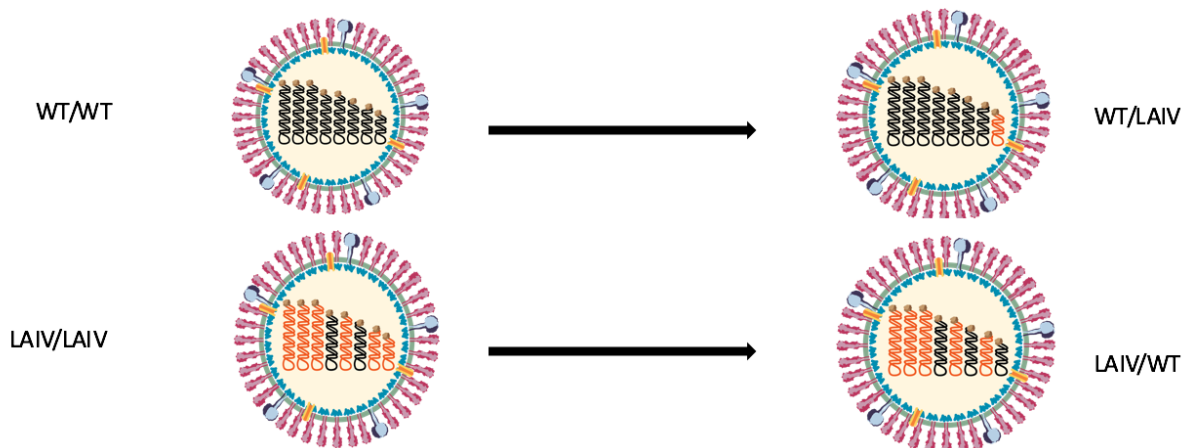| | Lineage of Segments 1-7 | Lineage of NS Segment | Abbreviation |
|---|---|---|---|
| 1 | A/Victoria/361/2011 | A/Victoria/361/2011 | WT/WT |
| 2 | A/Victoria/361/2011 | LAIV | WT/LAIV |
| 3 | LAIV | LAIV | LAIV/LAIV |
| 4 | LAIV | A/Victoria/361/2011 | LAIV/WT |

Table 3. 7:1 Virus Panel



Figure 9. Representation of 7:1 NS Gene Swaps between wt A/Victoria/361/2011 and LAIV

28

Since the NS segment encodes two proteins, NS1 and NEP, sequence alignments of wild type A/Victoria/361/2011 and LAIV NS1 and NEP were performed in order to examine amino acid differences. There are 28 discrete amino acid differences between the wild type and LAIV NS1 proteins. In regards to NEP, there are 7 discrete amino acid differences. When used in our NS reassortant virus system, this variation in amino acids between the protein sequences might shed light on LAIV attenuation.



Figure 10. Sequence Alignment of wild type A/Victoria/361/2011 and LAIV NS1
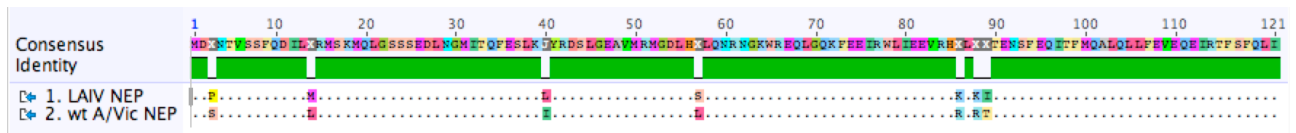


Figure 11. Sequence Alignment of wild type A/Victoria/361/2011 and LAIV NEP

## 2.2 Materials and Methods

### 2.2.1 Cell Lines

Madin-Darby canine kidney (MDCK) cells were maintained in Dulbecco's Modified Eagle's Medium (DMEM) with 10% fetal bovine serum (FBS), 100 U/mL penicillin, 100 ug/mL streptomycin and 2mM L-glutamine at 37$^{\circ}$C with 5% $CO_2$ and passaged at a 1:10 dilution every 3-4 days.

the WT/WT virus, however both reached roughly the same peak titer at 72 hours post infection (Fig. 13).
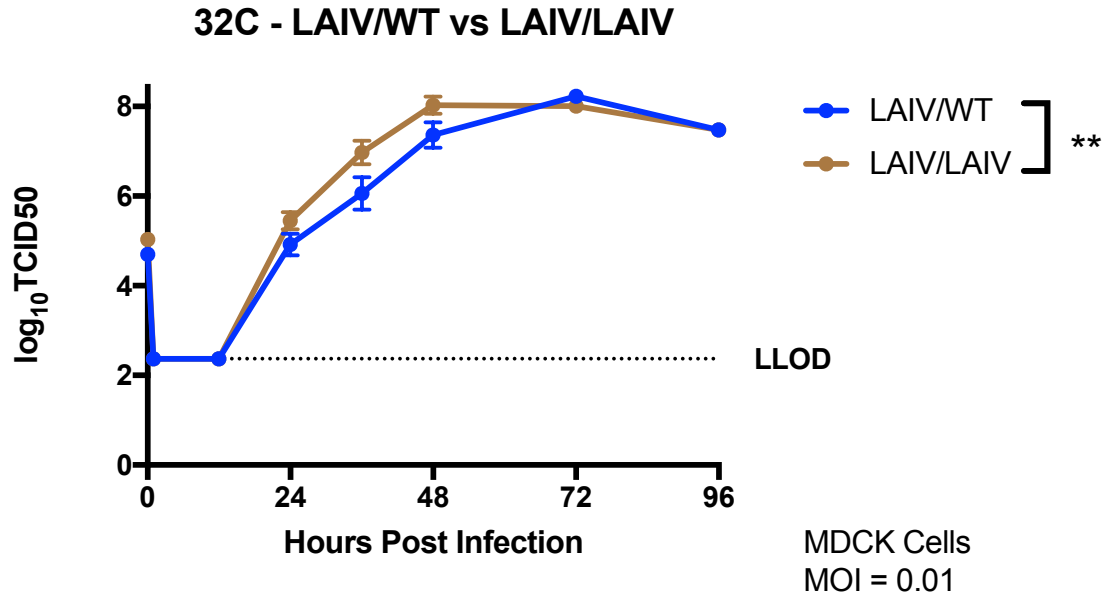
## 32C - LAIV/WT vs LAIV/LAIV



Figure 12. Effect of NS Gene Swap in the LAIV backbone at $32^{o}C$ in MDCK Cells. A multistep growth curve was performed on MDCK cells with the indicated viruses. Statistical differences were determined by MANOVA followed by Bonferroni post-test. *=P < 0.05; **= P < 0.01; ***=P<0.001. L.O.D=limit of detection=2.37.

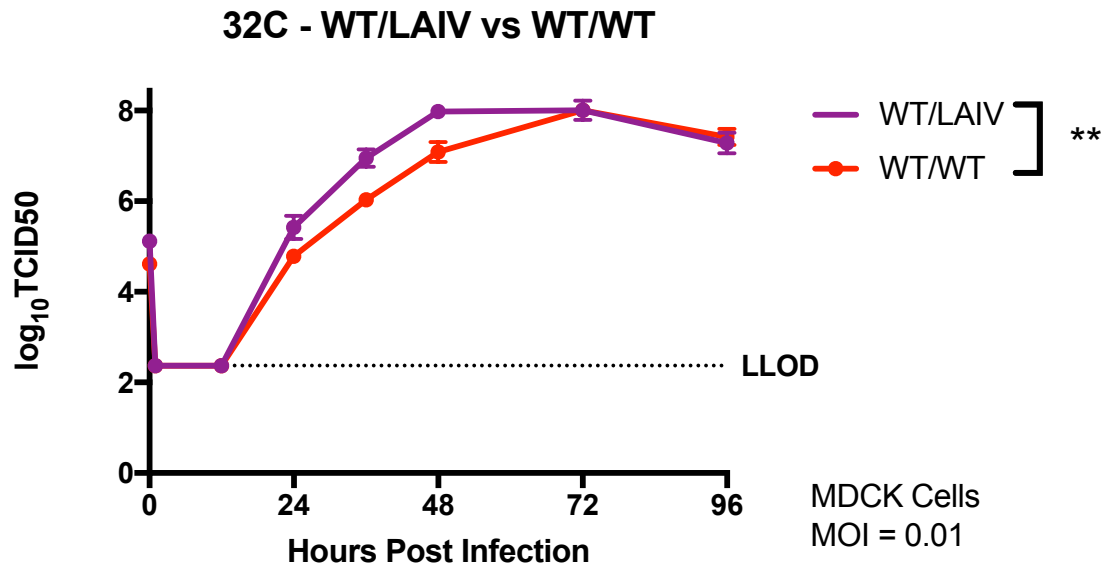**32C - WT/LAIV vs WT/WT**

Figure 13. Effect of NS Gene Swap in the A/Victoria/361/2011 backbone at $32^{o}$C in MDCK Cells. A multistep growth curve was performed on MDCK cells with the indicated viruses. Statistical differences were determined by MANOVA followed by Bonferroni post-test. *=P < 0.05; **= P < 0.01; ***=P<0.001. L.O.D=limit of detection=2.37.

## 2.3.3 Replication of NS Reassortant Viruses at $37^{o}$C in MDCK Cells

A multistep growth curve was also performed at $37^{o}$C to mimic an infection of the lower respiratory tract, which is also representative of core body temperature. Once again, the LAIV/LAIV virus had significantly faster replication kinetics than LAIV/WT, but both viruses achieved roughly the same peak titer at 48 hours post infection (Fig. 14). Additionally, the WT/LAIV virus had significantly faster replication kinetics than the WT/WT virus, however both strains reached roughly the same peak titer at 48 hours post infection (Fig. 15).
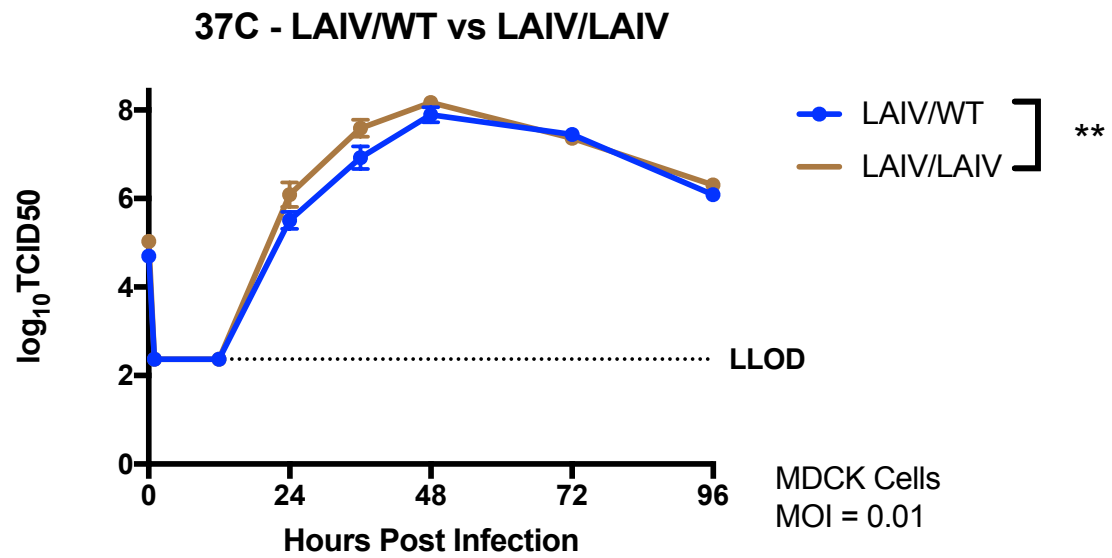
**37C - LAIV/WT vs LAIV/LAIV**

Figure 14. Effect of NS Gene Swap in the LAIV backbone at 37°C in MDCK Cells. A multistep growth curve was performed on MDCK cells with the indicated viruses. Statistical differences were determined by MANOVA followed by Bonferroni post-test. *=P < 0.05; **= P < 0.01; ***=P<0.001. L.O.D=limit of detection=2.37.

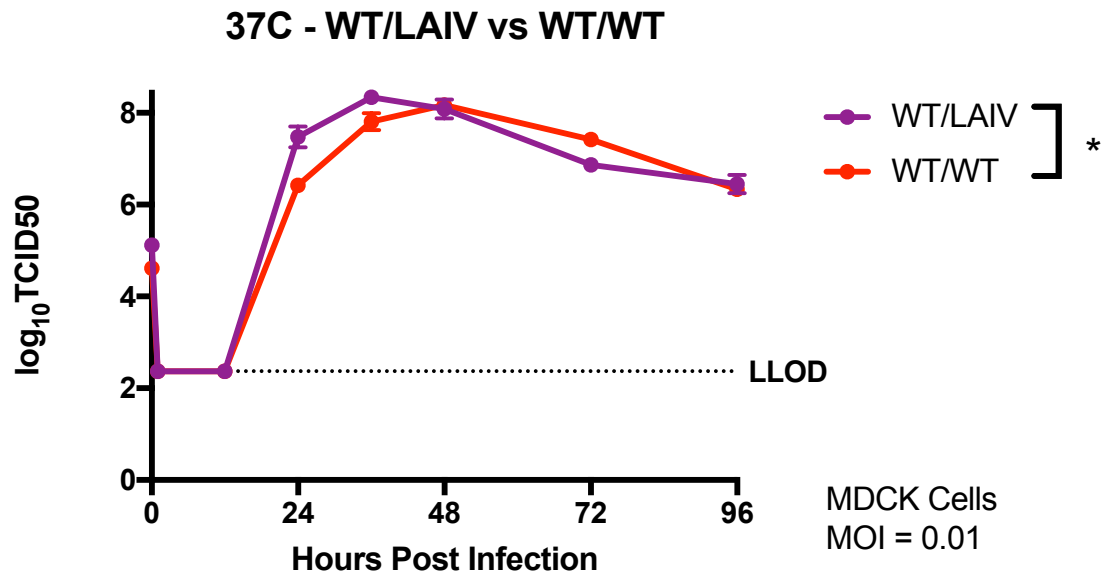**37C - WT/LAIV vs WT/WT**

Figure 15. Effect of NS Gene Swap in the A/Victoria/361/2011 backbone at $37^{\circ}C$ in MDCK Cells. A multistep growth curve was performed on MDCK cells with the indicated viruses. Statistical differences were determined by MANOVA followed by Bonferroni post-test. *=P < 0.05; **= P < 0.01; ***=P<0.001. L.O.D=limit of detection=2.37.

## 2.3.4 Replication of NS Reassortant Viruses at $32^{\circ}C$ in A549 Cells

A549 cells were infected to further evaluate viral growth kinetics for the NS reassortant viruses. Originating from adenocarcinomic alveolar basal epithelial cells, A549s present a more humanized model for influenza infection than MDCK cells. The A549 cells were infected at an MOI = 0.55.

A multistep growth curve was performed at $32^{\circ}C$. For the viruses in the LAIV backbone, the LAIV/LAIV and LAIV/WT viruses show no significant difference in replication kinetics – both viruses reached roughly the same peak titer at a similar rate (Fig. 16). For the viruses in the A/Victoria/361/2011 backbone, the WT/LAIV virus reached a peak titer nearly 100-fold greater than its WT/WT counterpart. Furthermore, the WT/LAIV virus reached its peak titer at a faster rate than the WT/WT virus (Fig. 17).
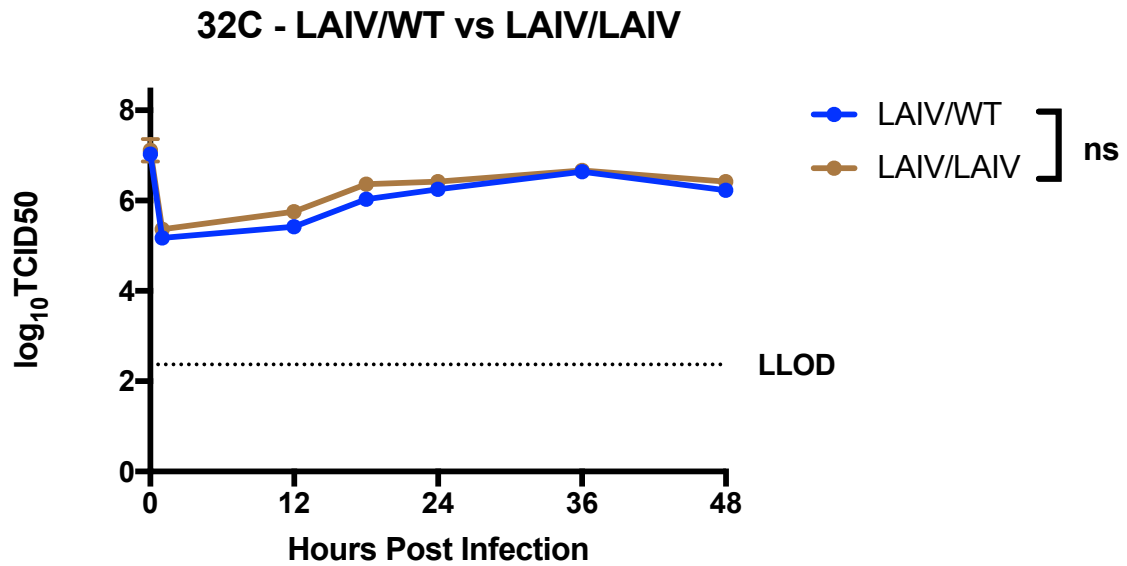
38

**32C - LAIV/WT vs LAIV/LAIV**

Figure 16. Effect of NS Gene Swap in the LAIV backbone at $32^{o}$C in A549 Cells. A multistep growth curve was performed on MDCK cells with the indicated viruses. Statistical differences were determined by MANOVA followed by Bonferroni post-test. *=P < 0.05; **= P < 0.01; ***=P<0.001. L.O.D=limit of detection=2.37.

Figure 17. Effect of NS Gene Swap in the A/Victoria/361/2011 backbone at $32^{o}C$ in A549 Cells. A multistep growth curve was performed on MDCK cells with the indicated viruses. Statistical differences were determined by MANOVA followed by Bonferroni post-test. *=P < 0.05; **= P < 0.01; ***=P<0.001. L.O.D=limit of detection=2.37.
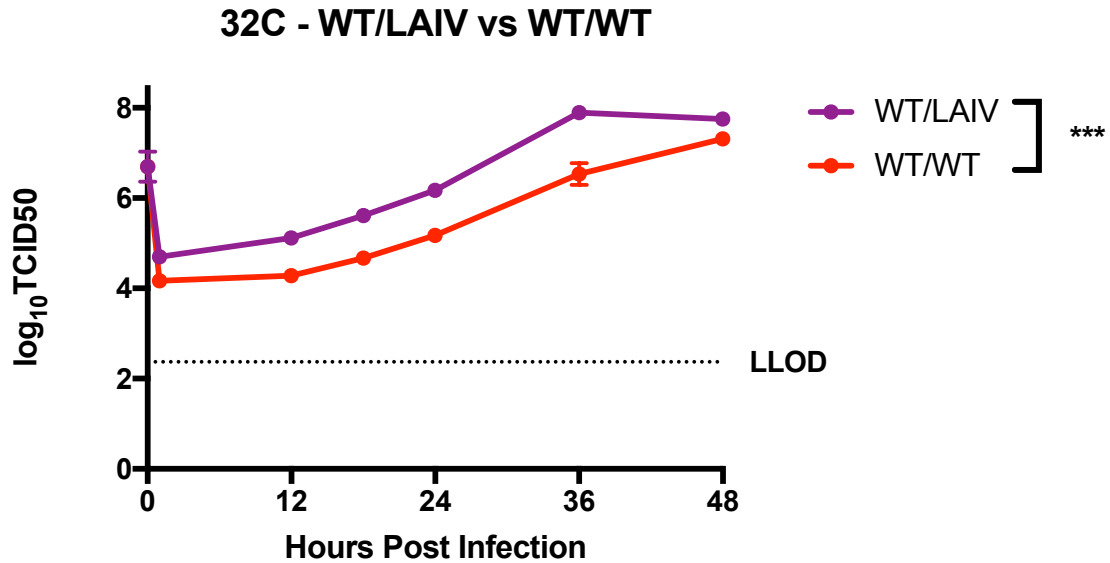
### 2.3.5 Replication of NS Reassortant Viruses at $37^{o}C$ in A549 Cells

Multistep growth curves were also performed at $37^{o}C$ to evaluate any temperature sensitive phenotypes in the virus panel. The A549 cells were inoculated at an MOI = 0.55.

Similar to what was observed at $32^{o}C$, the LAIV/LAIV and LAIV/WT viruses demonstrated no significant differences in replication kinetics at $37^{o}C$ (Fig. 18). They both reached roughly the same peak titer in the same amount of time. For the WT viruses, however, the WT/LAIV virus reached its peak titer faster than the WT/WT virus. Both viruses achieved roughly the same peak titer (Fig. 19).
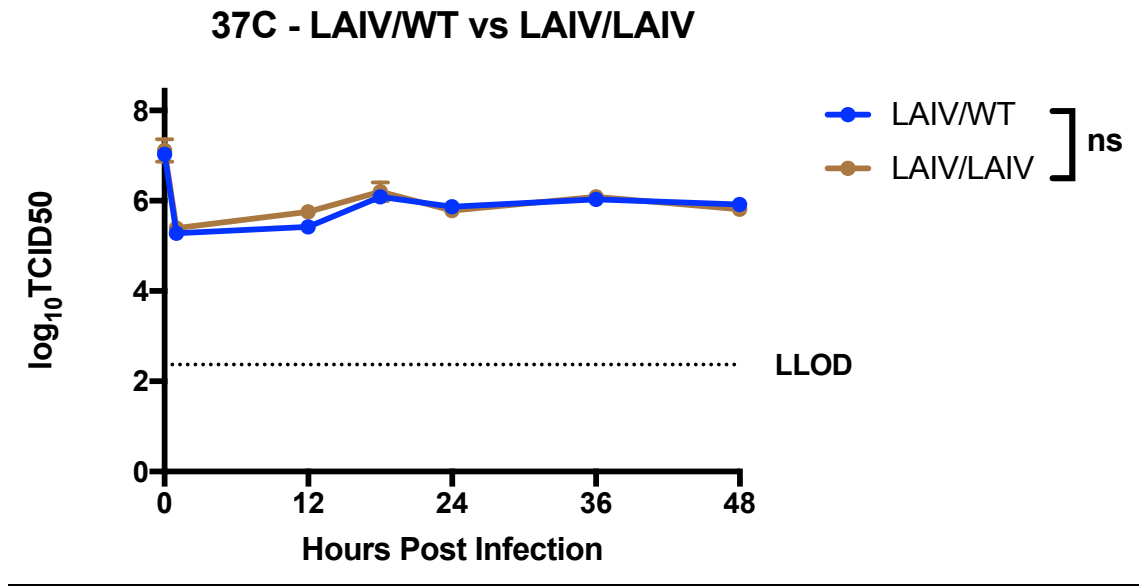
**37C - LAIV/WT vs LAIV/LAIV**

Figure 18. Effect of NS Gene Swap in the LAIV backbone at 37$^o$C in A549 Cells. A multistep growth curve was performed on MDCK cells with the indicated viruses. Statistical differences were determined by MANOVA followed by Bonferroni post-test. *=P < 0.05; **= P < 0.01; ***=P<0.001. L.O.D=limit of detection=2.37.

## 37C - WT/LAIV vs WT/WT

Figure 19. Effect of NS Gene Swap in the A/Victoria/361/2011 backbone at 37$^{o}$C in A549 Cells. A multistep growth curve was performed on MDCK cells with the indicated viruses. Statistical differences were determined by MANOVA followed by Bonferroni post-test. *=P < 0.05; **= P < 0.01; ***=P<0.001. L.O.D=limit of detection=2.37.
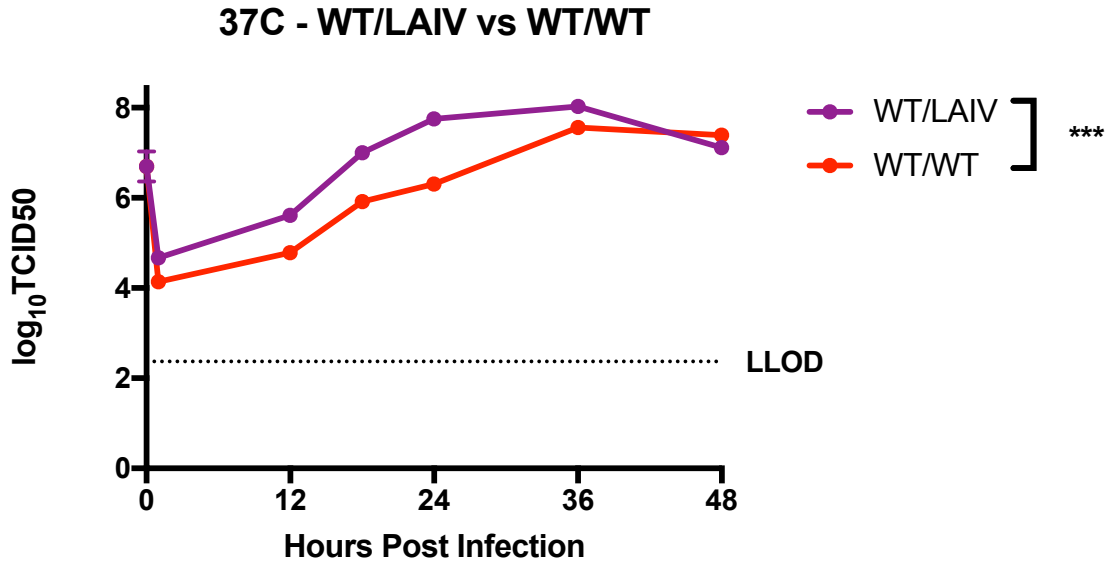
## *2.4 Discussion*

Previous work suggests that mutations which arise in the NS gene during the serial passage process of LAIV may contribute to viral attenuation and/or temperature sensitivity [66]. We examined this through NS gene segment reassortments in a panel of viruses. Although this does not allow us to determine the specific mutations that may contribute to an attenuation phenotype, we would be able to determine what role, if any, the entire gene segment has in viral replication. To test this, we performed several multistep growth curves between the NS reassortant viruses outlined in Table 3.

In MDCK cells at a low MOI (MOI = 0.01), there were significant differences between LAIV/LAIV and LAIV/WT, as well as significant differences between WT/LAIV and WT/WT. In both backbones, the virus with the LAIV NS gene segment had faster

the wt A/Ann Arbor/6/60 A153 genotype, LAIV's T153 genotype, and the avian D153 genotype. These viruses are listed in Tables 4 and 5.

| Mutation | Amino Acid | Properties | Structure of Functional Group |
|---|---|---|---|
| E153A | Alanine | Nonpolar, hydrophobic | H₃C—— |
| E153T | Threonine | Polar, uncharged | H₃C—CH—, OH |
| E153D | Aspartic Acid | Acidic | ⁻O—C(=O)—CH₂— |

Table 4. Panel of aa 153 Viruses in A/Victoria/361/2011 Backbone

| Mutation | Amino Acid | Properties | Structure of Functional Group |
|---|---|---|---|
| T153A | Alanine | Nonpolar, hydrophobic | H₃C—— |
| T153E | Glutamic Acid | Acidic | ⁻O—C(=O)—CH₂—CH₂— |
| T153D | Aspartic Acid | Acidic | ⁻O—C(=O)—CH₂— |

Table 5. Panel of aa 153 Viruses in LAIV Backbone

| Influenza Strain | Amino Acid | Frequency (%) |
|---|---|---|
| Human H1N1 | Glutamic Acid | 99 |
| Human H3N2 | Glutamic Acid | 99 |
| Avian (all subtypes) | Glutamic Acid | 23 |
| | Aspartic Acid | 76 |

Table 6. Frequency of Amino Acids Isolated from North American Clinical Samples (aa 153)

## 3.2 Materials and Methods

### 3.2.1 Cell Lines

Madin Darby canine kidney (MDCK) cells were maintained in Dulbecco's Modified Eagle's Medium (DMEM) with 10% fetal bovine serum (FBS), 100 U/mL penicillin, 100 ug/mL streptomycin and 2mM L-glutamine at $37^{o}C$ with 5% $CO_2$ and passaged at a 1:10 dilution every 3-4 days.

Transformed human embryonic kidney 293 cells (293T) were maintained in DMEM with 10% fetal bovine serum (FBS), 100 U/mL penicillin, 100 ug/mL streptomycin and 2mM L-glutamine at $37^{o}C$ with 5% $CO_2$ and passaged at a 1:10 dilution every 3-4 days.

### 3.2.2 Plasmids

| Plasmid | Forward Primer | Reverse Primer |
|---|---|---|
| pHH21 A/Vic-NS1-E153A | 5' CCA ACA ATT GCT CCG GCT TCG GTG AAA GCC CTT AGT AAT ACT AT 3' | 5' ATA GTA TTA CTA AGG GCT TTC ACC GAA GCC GGA GCA ATT GTT GG 3' |
| pHH21 A/Vic-NS1-E153D | 5' CCA ACA ATT GCT CCG TCT TCG GTG AAA GCC CTT AGT AAT ACT AT 3' | 5' ATA GTA TTA CTA AGG GCT TTC ACC GAA GAC GGA GCA ATT GTT GG 3' |
| pHH21 A/Vic-NS1-E153T | 5' CCA ACA ATT GCT CCC GTT TCG GTG AAA GCC CTT AGT AAT ACT AT 3' | 5' ATA GTA TTA CTA AGG GCT TTC ACC GAA ACG GGA GCA ATT GTT GG 3' |
| pHH21 LAIV-NS1-T153A | 5' CCA ACA ATT GCT CCG GCT TCG GTG AAA GCC CTT AGT AAT AAT AT 3' | 5' CTA ATA TTA CTA AGG GCT TTC ACC GAA GCC GGA GCA ATT GTT GG 3' |
| pHH21 LAIV-NS1-T153D | 5' CCA ACA ATT GCT CCG TCT TCG GTG AAA GCC CTT AGT AAT ATT AT 3' | 5' CTA ATA TTA CTA AGG GCT TTC ACC GAA GAC GGA GCA ATT GTT GG 3' |
| pHH21 LAIV-NS1-T153E | 5' CCA ACA ATT GCT CCC TCT TCG GTG AAA GCC CTT AGT AAT ATT AT 3' | 5' CTA ATA TTA CTA AGG GCT TTC ACC GAA GAG GGA GCA ATT GTT GG 3' |

Table 7. Sequences of Primers used to Generate Recombinant Viruses at aa 153

### 3.2.3 Recombinant Viruses

A 12 plasmid recombinant virus rescue system was utilized to generate the panel viruses (Neumann et al., 1999). 6-well plates were coated with poly-L-lysine and 293T cells were plated at 40-60% confluence 24 hours prior to transfection. For the A/Victoria/361/2011 viruses, 293T cells were transfected with A/Victoria/361/2011 pHH21 plasmids encoding PB2, PB1, PA, NP, NA, HA, M (0.5 µg each) and NS (1.0 µg). For the

# Curriculum Vitale

# James E. Stanton

**307 Sheep Pasture Rd., Waynesville, NC 28785 ● (828) 400-9468 ●
jstanton828@gmail.com**

---

## EDUCATION

**Johns Hopkins Bloomberg School of Public Health, Baltimore, MD**
- *Master of Science (ScM)*, May 2017; GPA 3.75/4.0
- *Concentration:* Molecular Microbiology and Immunology
- *Research Focus:* Studied the Live Attenuated Influenza Vaccine virus and the influence of its NS1 protein on viral replication and inhibition of host innate immune responses

**University of North Carolina Asheville, Asheville, NC**
- *Bachelor of Science in Chemistry*, May 2014; GPA 3.23/4.0
- *Concentration:* Biochemistry
- *Honors*: University Scholar, University Research Scholar, Deans List Spring 2012, Laurels Scholar

## EMPLOYMENT HISTORY

**Occupational Health Technician**                                      Feb. 2014 - Aug. 2015
Pardee Urgent Care, Hendersonville, NC
- Triaged and communicated patient's chief complaint/medical history to providers
- Executed basic laboratory procedures including strep throat and flu tests, casting of strained/broken limbs, administration of EKGs, cleaning and dressing of wounds, etc.
- Administered urine drug screens and breath alcohol tests to business and industry clients
- Obtained certification in Basic Life Support.

**Undergraduate Research Associate**                                      May 2012 - May 2014
UNC Asheville, Asheville, NC
- Undertook original, student-driven research that focused on synthesizing phenstatin analogues - a group of molecules believed to inhibit cancer cell division.
- Techniques utilized included: reflux, aldol condensation, Hemetsberger-Knittel thermolysis, silica gel column chromatography, various workup and separatory techniques for compound purification, and analysis via infrared, proton NMR, and carbon NMR spectroscopy
- Research published in the 2014 UNC Asheville Journal of Undergraduate Research

**Student Events Coordinator**                                      October 2011- May 2013
UNC Asheville Alumni Relations, Asheville, NC
- Assisted in preparation and set-up of events for Alumni Relations including gathering materials and preparing handouts/informational materials for the event
- Networked with area alumni to re-establish connections with the university and to aid in raising